

**PLIO-PLEISTOCENE DEPOSITIONAL SEQUENCES
OF THE SOUTHWESTERN LOUISIANA CONTINENTAL SHELF AND SLOPE:
GEOLOGIC FRAMEWORK, SEDIMENTARY FACIES,
AND HYDROCARBON DISTRIBUTION**

by

R. A. Morton and W. B. Ayers, Jr.

assisted by

A. M. Belasco, G. Marton, B. Sterrenberg, and G. F. Wick

**An industry sponsored research project supported by BP Exploration Inc., CNG
Producing Company, Fairfield Industries, Halliburton Geophysical Services, Mobil
Exploration and Producing US Inc., Oryx Energy Company, and Union Texas Petroleum.**

**Bureau of Economic Geology
W. L. Fisher, Director
The University of Texas at Austin
Austin, Texas 78713-7508**

1991

CONTENTS

ABSTRACT	1
INTRODUCTION	2
Regional Setting.....	2
Sources of Data.....	4
Electric Logs.....	4
Paleontology Reports.....	7
Seismic Profiles.....	9
Climate and Eustatic Fluctuations.....	11
Pliocene-Pleistocene Boundary.....	12
STRUCTURAL FRAMEWORK	12
Principal Structural Features.....	14
Extensional Faults.....	14
Shale and Salt Diapirs.....	16
Unconformities.....	19
Structural Styles.....	19
Timing of Structural Movement.....	23
DEPOSITIONAL SYSTEMS, SYSTEMS TRACTS, AND GENETIC SEQUENCES	24
Depositional Systems.....	24
Shelf-edge Delta Systems.....	24
Slope Systems.....	26
Depositional Systems Tracts.....	30
Sequence Boundaries and Offshore Sequences.....	32
Onshore Formations.....	33
PLIO-PLEISTOCENE STRATIGRAPHIC FRAMEWORK	34
Mapping Depositional Systems and Shelf Margins.....	35
Characteristics of Plio-Pleistocene Genetic Sequences.....	37
Pre- <u>Robulus</u> E (not mapped).....	37
<u>Robulus</u> E to <u>Buliminella</u> 1 (Unit 1).....	38
<u>Buliminella</u> 1 to <u>Globoquadrina altispira</u> (Unit 2).....	41
<u>Globoquadrina altispira</u> to <u>Lenticulina</u> 1 (Unit 3).....	46
<u>Lenticulina</u> 1 to <u>Angulogerina</u> B (Unit 4).....	49
<u>Angulogerina</u> B to <u>Hyalinea balthica</u> (Unit 5).....	53
<u>Hyalinea balthica</u> to <u>Trimosina</u> A (Unit 6).....	57
<u>Trimosina</u> A to <u>Globorotalia flexuosa</u> (Unit 7).....	60
post- <u>Globorotalia flexuosa</u> (Unit 8).....	64

SUMMARY OF DEPOSITIONAL AND STRUCTURAL HISTORY	64
Late Miocene and Early Pliocene (6.0 Ma - 3.7 Ma).....	64
Middle Pliocene (3.7 Ma - 2.8 Ma).....	66
Late Pliocene (2.8 Ma - 2.2 Ma).....	67
Early Pleistocene (2.2 Ma - 1.5 Ma).....	68
Middle Pleistocene (1.5 Ma - 0.65 Ma).....	69
Late Pleistocene (0.65 Ma - present).....	70
HYDROCARBON GENERATION AND DISTRIBUTION.....	72
Source Rock Potential, Thermal Maturation, and Petroleum Migration.....	72
Spatial Distribution of Hydrocarbons.....	74
Delineation of Hydrocarbon Plays.....	77
Play Characteristics and Exploration Potential.....	82
Play 1.....	84
Play 2.....	85
Play 3.....	86
Play 4.....	88
Play 5.....	89
Play 6.....	90
SUMMARY AND CONCLUSIONS	92
ACKNOWLEDGMENTS.....	96
REFERENCES	98
APPENDIX: Plio-Pleistocene Recoverable Reserves and Cumulative Field Production	112

FIGURES

1. Chronostratigraphic and biostratigraphic subdivision of Plio-Pleistocene strata in the western Gulf Coast Basin.....	5
2. Schematic cross section of Plio-Pleistocene strata in the West Cameron and western Garden Banks areas showing the lithologic and biostratigraphic criteria used to correlate genetic sequences.....	6
3. Regional depositional framework of Plio-Pleistocene strata.....	oversize
4. Structural features of the southwestern Louisiana continental shelf and slope, Plio-Pleistocene productive trend.....	oversize

5. Structural cross section derived from seismic profile illustrating lithofacies, stratigraphic subdivisions, and structural style in the northern sector of the study area.....oversize
6. Structural cross section derived from seismic profile illustrating lithofacies, stratigraphic subdivisions, and structural style near the eastern margin of the study area.....oversize
7. Structural cross section derived from seismic profile illustrating lithofacies, stratigraphic subdivisions, and structural style near the center of the study area.....oversize
8. Structural cross section derived from seismic profile illustrating lithofacies, stratigraphic subdivisions, and structural style near the western margin of the study area.....oversize
9. Structural cross section derived from seismic profile illustrating lithofacies, stratigraphic subdivisions, and structural style of the upper continental slope.....oversize
10. Typical electric log responsesoversize
11. Net sandstone map of unit 1 (Robulus E to Buliminella 1)oversize
12. Percent sandstone map of unit 1 ((Robulus E to Buliminella 1)oversize
13. Depositional systems map of unit 1 ((Robulus E to Buliminella 1)oversize
14. Net sandstone map of unit 2 (Buliminella 1 to Globoquadrina altispira)oversize
15. Percent sandstone map of unit 2 (Buliminella 1 to Globoquadrina altispira)oversize
16. Depositional systems map of unit 2 (Buliminella 1 to Globoquadrina altispira)oversize
17. Net sandstone map of unit 3 (Globoquadrina altispira to Lenticulina 1)oversize
18. Percent sandstone map of unit 3 (Globoquadrina altispira to Lenticulina 1)oversize
19. Depositional systems map of unit 3 (Globoquadrina altispira to Lenticulina 1)oversize
20. Net sandstone map of unit 4 (Lenticulina 1 to Angulogerina B)oversize
21. Percent sandstone map of unit 4 (Lenticulina 1 to Angulogerina B)oversize
22. Depositional systems map of unit 4 (Lenticulina 1 to Angulogerina B)oversize
23. Composite net sandstone map for pre-Hyalinea balthica sand-rich submarine fans penetrated in the northern Garden Banks areaoversize

24.	Net sandstone map of unit 5 (<u>Angulogerina B</u> to <u>Hyalinea balthica</u>)	oversize
25.	Percent sandstone map of unit 5 (<u>Angulogerina B</u> to <u>Hyalinea balthica</u>)	oversize
26.	Depositional systems map of unit 5 (<u>Angulogerina B</u> to <u>Hyalinea balthica</u>)	oversize
27.	Net sandstone map of unit 6 (<u>Hyalinea balthica</u> to <u>Trimosina A</u>).....	oversize
28.	Percent sandstone map of unit 6 (<u>Hyalinea balthica</u> to <u>Trimosina A</u>).....	oversize
29.	Depositional systems map of unit 6 (<u>Hyalinea balthica</u> to <u>Trimosina A</u>).....	oversize
30.	Net sandstone map of unit 7 (<u>Trimosina A</u> to <u>Globorotalia flexuosa</u>)	oversize
31.	Percent sandstone map of unit 7 (<u>Trimosina A</u> to <u>Globorotalia flexuosa</u>)	oversize
32.	Depositional systems map of unit 7 (<u>Trimosina A</u> to <u>Globorotalia flexuosa</u>)	oversize
33.	Distribution of Plio-Pleistocene oil and gas fields and their subdivision into principal exploration plays	oversize
34.	Sizes of known Plio-Pleistocene oil and gas fields in the West Cameron and western Garden Banks areas.....	76
35.	Cumulative production and recoverable reserves for each Plio-Pleistocene play in the West Cameron and western Garden Banks areas.....	81

TABLE

1.	Summary of geologic characteristics and remaining exploration potential of Plio-Pleistocene hydrocarbon plays in the West Cameron and western Garden Banks areas	78
----	--	----

PLATES

- I. Structural cross section 1'-1''
- II. Structural cross section 2'-2''
- III. Structural cross section 3'-3''

ABSTRACT

The Plio-Pleistocene hydrocarbon fairway of offshore Louisiana is restricted to the outer continental shelf and upper continental slope where a thick wedge of nearshore and deep marine sediments was deposited. Electric logs, paleontological reports, and seismic profiles form the basis for (1) dividing the wedge of Plio-Pleistocene strata into eight genetic sequences, (2) establishing the structural framework, (3) determining the timing of deformation, and (4) mapping the principal depositional systems of the West Cameron and western Garden Banks areas during the past five million years. Sedimentary facies and structural styles in this part of the Gulf Coast basin are highly variable owing to contemporaneous sea-level fluctuations, salt migration, and shifting sites of deltaic, shelf and slope sedimentation. The resulting complex geologic history of this part of the basin was interpreted to determine what controlled the generation, migration, and entrapment of hydrocarbons.

The early Pliocene was a period of continental platform inundation and deposition of a thick succession of marine mudstones. About 3 Ma this monotonous accumulation of deep-water mudstone was interrupted by deposition of sand-rich submarine channels and fans associated with a lowering of sea level. These lowstand deposits extended at least 55 mi (90 km) basinward of the paleomargin. Overlying Pleistocene sediments were deposited mainly by prograding mud-rich fluvial-deltaic systems of moderate size. These rivers and shelf-edge deltas constructed a broad continental platform that buried the submarine fans and prograded the shelf margin approximately 70 mi (110 km) basinward. During this rapid outbuilding, slumping and other gravity-driven mass transport processes removed sand-rich delta-front sediments from unstable shelf margins and redeposited them on the continental slope.

Plio-Pleistocene reservoirs in the West Cameron and western Garden Banks areas contain more than 1.1 billion barrels of oil equivalent in at least 100 different fields or local accumulations. Most of the fields are located near faults associated with late salt movement although a few fields are located near shallow salt diapirs. Salt is normally preserved at great depth in thin sheets beneath listric faults or is absent as a result of prolonged evacuation. The fields are grouped into six exploration plays on the basis of structural style, reservoir facies, and hydrocarbon composition. The most prolific play is characterized by stacked delta-front reservoirs producing from broad rollover anticlines that formed in a graben complex between the Trimosina regional and counter-regional fault systems. Each play primarily produces gas although some oil is produced from fields beneath the continental slope. New field discoveries or reserve growth are likely in all six plays as a result of deeper drilling or off-structure exploration in former intraslope sub-basins.

Keywords: genetic sequence, depositional system, Gulf Coast, hydrocarbons, Plio-Pleistocene, offshore Louisiana

INTRODUCTION

Regional Setting

The Texas-Louisiana outer continental shelf and slope comprise the last large frontier for hydrocarbon exploration in the northern Gulf of Mexico. By industry standards this is a relatively young productive trend since active drilling in relatively deep water began only a few decades ago. Before significant Plio-Pleistocene discoveries were made, this frontier province was considered unfavorable for petroleum

exploration because the sediments are geologically young and thermally immature and were thought to be deficient in sandstone reservoirs, and thus severely limited in their potential to generate and store hydrocarbons.

As exploration of the outer continental shelf matured, the search for significant Plio-Pleistocene reserves focused on the adjacent continental slope. In this deep-water play, known as the flexure trend, salt structures and sand-rich turbidites have combined to trap significant accumulations of hydrocarbons. Interest in the deep-water play has continued to be stimulated by the discovery of substantial oil and gas reserves on the middle continental slopes of Louisiana and Texas. More recently, frontier exploration leasing has shifted to extremely deep water (more than 8,000 ft. [2,440 m] deep) as a result of new concepts of salt deformation and new strategies for exploring beneath the sheets of allochthonous salt. Turbidites of late Neogene or Quaternary age are the primary exploration targets in this deep-water subsalt play.

Reservoir-quality sands present in the Mississippi fan (Bouma and others, 1985) and in a Miocene abyssal plain fan (Stuart and Caughey, 1977) are encouraging evidence that similar sand-rich turbidites are present upslope of the abyssal plain. Recent drilling in water more than 4,000 ft (1,200 m) deep has confirmed the presence of Plio-Pleistocene sand-rich submarine fans that will extend the search for oil and gas farther basinward. Only the extremely high costs of production at these water depths have prevented development of new reserves discovered on the middle slope.

The regional geologic setting and general history of the Plio-Pleistocene producing trend in the western Gulf Coast Basin have been previously described (Woodbury and others, 1973; Caughey, 1975; Poag and Valentine, 1976; Sheffield, 1978). A few

published reports provide details about local structures, paleontological zones, hydrocarbon traps and facies changes (Stude, 1984; Reed and others, 1987; Austin, 1988; Hidle and Wright, 1988), but no regional maps have been published that emphasize stratigraphic sequences, sand distribution, and hydrocarbon plays in the West Cameron and western Garden Banks areas.

The primary purposes of this study are to: (1) describe the structural and stratigraphic frameworks of Plio-Pleistocene strata in southwestern offshore Louisiana, (2) determine the dependencies among hydrocarbon reservoirs, genetic sequences, and depositional systems tracts, and (3) evaluate the remaining exploration potential of the region. This was accomplished by extending interpreted cross sections from the adjacent High Island and East Breaks areas (Morton and Jirik, 1989; Morton and others, 1991) into the West Cameron and western Garden Banks areas, mapping the principal Plio-Pleistocene genetic sequences (figs. 1 and 2) and related depositional systems, interpreting their geologic histories, and summarizing the physical attributes of the associated hydrocarbon plays.

Sources of Data

Electric Logs

A principal database for this study was approximately 270 geophysical logs of wells penetrating part or all of the Plio-Pleistocene section. These well logs were correlated to prepare regional cross sections (Pls. 1-3) and supplementary subregional sections. The network of cross sections and a grid of regional seismic lines was used to establish the structural fabric and stratigraphic framework and to interpret the styles of intrabasinal deformation.

Series	Benthic markers	Map unit	Age (mya)	Relative change of coastal onlap		Systems tracts
				Landward	Basinward	
Pleistocene	<i>Globorotalia flexuosa</i> *	8	0.55		LSW	
	<i>Trimosina A</i> *	7			HST/TST	
	<i>Hyalinea balthica</i> *	6			LSW	
					HST	
					TST	
Pliocene	<i>Angulogerina B</i> *	5	1.0		TST	
			1.4		LSW	
			1.6		LSF	
	<i>Cristellaria S</i>	4	2.0		HST	
	<i>Lenticulina 1</i> *				TST	
					LSW	
				HST		
				TST		
Miocene	<i>Globoquadrina altispira</i> *	3	2.8	LSW		
			3.0	HST		
				TST		
	<i>Buliminella 1</i> *		3.7	LSW		
			4.0	LSF		
	<i>Robulus E</i>	1	5.2	HST		
				TST		

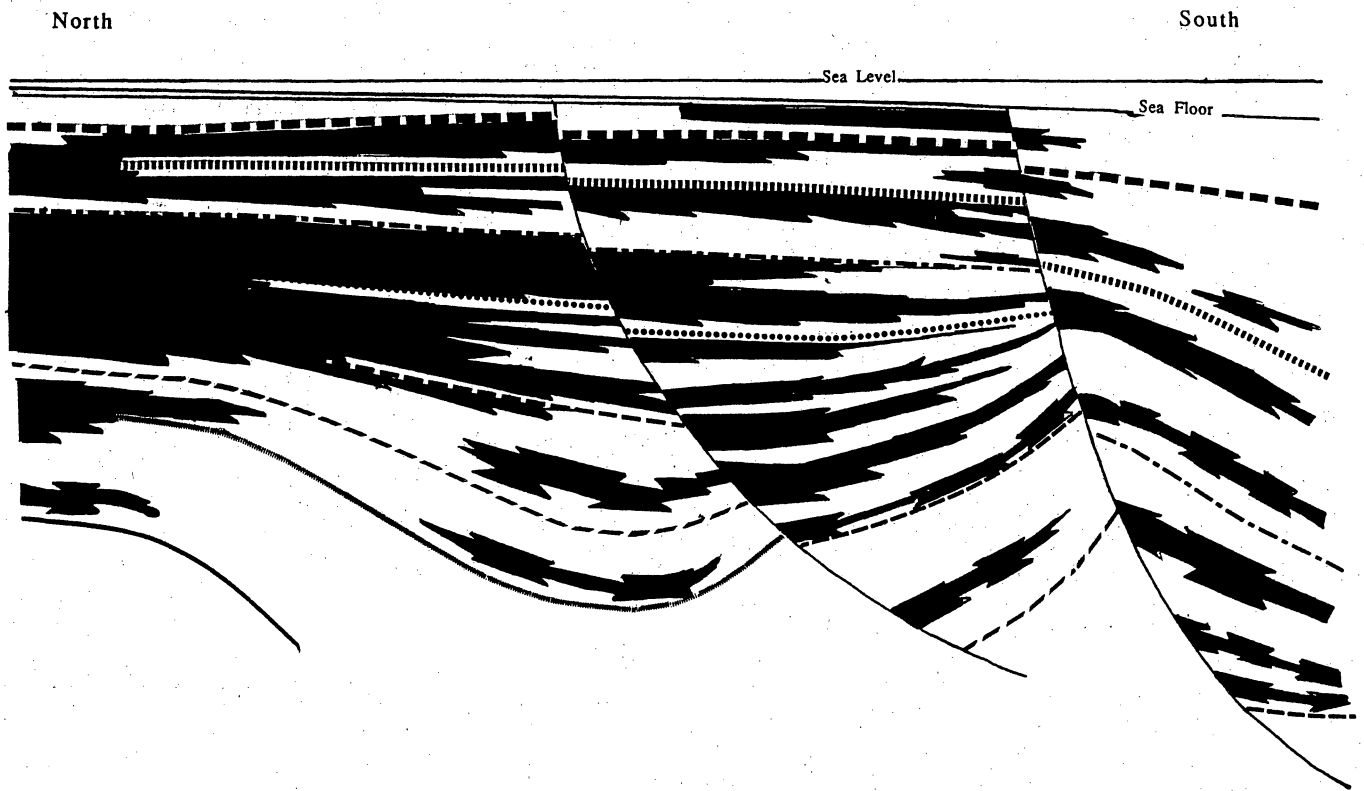
EXPLANATION

HST Highstand
 LSW Lowstand wedge
 TST Transgressive
 LSF Lowstand fan

* Mapping horizon

QA12857

Figure 1. Chronostratigraphic and biostratigraphic subdivision of Plio-Pleistocene strata in the western Gulf Coast Basin. The curve depicting relative changes of coastal onlap, presented by Beard and others (1982), and systems tracts designations, presented by Haq and others (1987), are included only for comparison with observed events. They were not used to map genetic sequences.



Explanation

<i>Globorotalia flexuosa</i>	— — — — —
<i>Trimosina A</i>
<i>Hyalinea balthica</i>	- - - - -
<i>Angulogerina B</i>
<i>Lenticulina 1</i>	- - - - -
<i>Globoquadrina altispira</i>
<i>Buliminella 1</i>	—————

Figure 2. Schematic cross section of Plio-Pleistocene strata in the West Cameron and western Garden Banks areas showing the lithologic and biostratigraphic criteria used to correlate genetic sequences.

Electric log patterns were used to interpret genetic facies and to reconstruct the lateral extent and attributes of the principal depositional systems. The log patterns were used with paleoecological information to determine depositional environments because continuous core samples of representative lithofacies were unavailable for examination. The electric log patterns represent the entire spectrum of sedimentary facies deposited in settings ranging from nonmarine to abyssal plain environments.

Paleontology Reports

Detailed paleontology reports or report summaries were obtained for approximately two-thirds of the wells used for correlation. These reports contain depths of extinction horizons for common benthic and planktonic foraminifers including some nannofossils. The report summaries also contain information about paleoecozones that can be used to infer paleobathymetry.

Correlation of some electric logs relied on lithostratigraphic markers rather than biostratigraphic markers because some reported extinction horizons in nearby wells appear to be out of place. Discrepancies in reported biostratigraphic tops can result from (1) changes in depositional environments over geologic time (facies changes cause updip suppression or downdip elevation of faunal occurrence), (2) sediment reworking and faunal displacement (first downhole occurrence is above the extinction horizon), (3) section omission (first downhole occurrence is below the extinction horizon because of erosional unconformity or faulting), (4) differences in sample quality and processing, and differences in well-sample interpretation by individual paleontologists. For purposes of regional mapping, these discrepancies are accommodated by using the most consistent biostratigraphic position reported for wells in the area.

In this study, the Angulogerina B (Ang B) horizon (figs. 1 and 2) is the least reliable biostratigraphic correlation marker for two reasons. First, the Ang B fauna appears progressively higher (climbs) in the section in updip wells. Locally the diachronous extinction may be environmentally controlled or it may be a result of uplift, erosion, and redeposition of the Ang B fauna. The Ang B marker is also difficult to use because the fauna is absent in downdip positions. The fauna is probably absent basinward of its paleo-shelf margin because the deep-water environment prevented habitation by the benthic foram.

Minor correlation problems occur where the extinction horizon of the planktonic foram Globorotalia miocenica (Glob m) is slightly below or above that of the benthic foram Lenticulina 1 (Lent 1). Because the benthic and planktonic forams are used as time equivalents, the slightly younger Glob m pick requires a slight adjustment of the mapping horizon.

Biofacies suppression of marker fossils can also cause minor discrepancies between electric log correlations and biostratigraphic horizons. Biofacies suppression occurs when time-equivalent beds deposited in shallow water do not contain the diagnostic species. In the southern West Cameron area, the Lent 1 top is suppressed because transitional brackish-water sandstones occupy the equivalent stratigraphic position. Glob miocenica is also missing from the updip sediments because the planktonic foram did not live in shallow water that prevailed as the shelf platform slowly subsided. In this same updip area, erosional contacts and obvious onlap are conspicuously absent above the Lent 1 map horizon, suggesting that the post-Lent 1 sediments are largely conformable or relief of merged unconformities is below the limit of seismic resolution.

Some paleontology reports use a conceptual glacial stage name (Basal Nebraskan) to represent the condensed section containing the extinction horizon of Globoquadrina altispira (Glob a). This substitution is supposedly justified because the faunal

extinction coincides with a period of accelerated cooling and expansion of continental glaciers in North America. In this report all mapping horizons are identified by paleontologic names to avoid confusing continental glacial terminology with subsurface Plio-Pleistocene sequence boundaries.

Seismic Profiles

A grid of recent high-quality multi-channel seismic lines, which covers more than 1,550 mi (2,100 km) of the study area, was interpreted using prominent seismic reflections. These strong reflections closely correspond to extinction horizons documented on well logs and in paleontology reports. Some of these mapped horizons also coincide with marine condensed sections as defined by Loutit and others (1988) and van Wagoner and others (1988). Seismic facies patterns were interpreted using the nomenclature and concepts reported by Sangree and Widmier (1977), Brown and Fisher (1977), Stuart and Caughey (1977), Sangree and others (1978), and Mitchum (1985).

Well-defined amplitude changes and reflection terminations, such as onlap, downlap, and truncation (Mitchum and others, 1977) are rarely observed on seismic lines used for this study. The structural overprint and shadow zones beneath faults mask many of the reported unconformable sequence boundaries (Haq and others, 1987) and obscure the details of stratal patterns at those boundaries. These limitations prevent mapping of stratigraphic units exclusively on the basis of seismic characteristics.

At the depositional (progradational) break in slope, or shelf margin (fig. 3), seismic characteristics change from variable-amplitude, parallel, nearly horizontal reflections to wavy or convex-upward clinoforms. Some changes in reflections are expressed as double inflection points seen along dip profiles. These inflection-point

couplets may represent gradient changes at the delta-plain/shoreface interface and at the shelf-edge/slope interface. Other seismic features used to identify shelf margins are the number, spacing, and displacement of contemporaneous faults and intraformational slumps signifying former unstable slopes.

Seismic facies patterns provide some highly interpretive criteria for predicting lithology. However, different lithologies can produce similar seismic responses. For example, simple genetic sequences commonly exhibit a systematic arrangement of five seismic facies that are products of the principal regressive-transgressive events. In coastal and shelf areas, (1) variable-amplitude, parallel to wavy, discontinuous reflections pass downward and basinward into (2) high-amplitude, parallel, continuous reflections. In turn, these reflection patterns and (3) low-angle oblique (clinoform) reflections pass downward and basinward into (4) variable-amplitude, discontinuous, hummocky and mounded reflections. These lowermost reflections are typically onlapped and overlain by (5) thin, high-amplitude, parallel drapes. This idealized seismic facies architecture corresponds to a progradational, upward-coarsening sequence of muddy outer shelf and upper slope slump deposits (seismic facies 4) overlain by interbedded muddy and sandy prodelta sediments (seismic facies 3) which, in turn, are overlain by sandy nearshore deposits (seismic facies 2) and interbedded sandy and muddy fluvial and coastal-plain deposits (seismic facies 1). After abandonment, the distal progradational wedge is onlapped by hemipelagic mud drapes (seismic facies 5) conforming to the abandonment surface.

Seismic expressions of deep-water deposits are somewhat different from those of the shallow water deposits. Upward-coarsening intraslope basin deposits are characterized by a basal, acoustically transparent zone overlain by parallel discontinuous reflections and an upper zone of thin, parallel continuous reflections.

This sequence represents coarse turbidites (sand and mud) overlain by widespread continuous drapes of pelagic and hemipelagic mud (Bouma, 1982).

The thickness of seismic sequences may help differentiate the types of deposits. For example, individual parasequences of intraslope basin fill typically are much thinner (<0.25 sec two-way travel time) than progradational wedges (0.5 to 1.0 sec two-way travel time) that constitute entire genetic sequences.

Climatic and Eustatic Fluctuations

During the Plio-Pleistocene Epoch, global temperatures fluctuated in response to changes in solar radiation that were driven by oscillations of the Earth's orbit (Frakes, 1979). Warmer temperatures melted continental ice sheets and raised sea level, whereas cooler temperatures had the opposite effect on the hydrosphere. At least eight major eustatic cycles have affected rates of sedimentation and loci of deposition in the northern Gulf of Mexico during the past 3.0 Ma (Beard and others, 1982).

Two episodes of intense glaciation permit correlation of continental glacial deposits with the deep marine record. The first significant glacial period was produced by pronounced cooling about 3.0 Ma when extensive glaciers formed in northern latitudes. Temperatures were coldest and sea level was lowest during this cooling trend about 2.4 Ma (Beard and others, 1982). The second episode of intense glaciation was caused by decreased temperatures about 1.6 Ma that initiated preceded a period of rapid temperature fluctuations and frequent shifts in coastal onlap (fig. 1)

Pliocene-Pleistocene Boundary

There is still disagreement regarding the age and biostratigraphic position of the Pliocene-Pleistocene boundary in the Gulf Coast Basin because different criteria can be used to define the boundary. Ages commonly given for the boundary include: (1) 2.8 Ma corresponding with a major climatic change, especially in the northern hemisphere (Beard and others, 1982), (2) 2.2 Ma coinciding with the extinction of Lenticulina 1 (Stude, 1984), (3) 1.85 Ma (Haq and others, 1987) to 1.75 Ma (Poag and Valentine, 1976) corresponding to the extinction of Discoaster brouweri, and (4) 1.66 Ma (Palmer, 1983) relying on radiometric correlation with the Italian type section.

Although it was not used as a mapping datum in this study, the Pliocene-Pleistocene boundary is placed at about 1.75 Ma (fig. 1). This age and stratigraphic position are defined on the basis of nannofossils in cores and well cuttings from the deep Gulf of Mexico and are accepted by most Gulf Coast stratigraphers.

STRUCTURAL FRAMEWORK

The Gulf Coast Basin formed by thermal relaxation and downwarping of oceanic crust after Mesozoic rifting of the Gulf of Mexico. The Plio-Pleistocene depocenter lies near the transitional boundary that separates basin-centered oceanic crust from rifted transitional crust underlying the shelf (Buffler and Sawyer, 1985). Beneath the outer shelf and slope, salt of variable thickness overlies presalt sediment and oceanic crust (Hall and others, 1983). Seismic profiles from the deep Gulf show that allochthonous salt sheets are being extruded over younger sediments near the Sigsbee Escarpment (Amery, 1969; Buffler and others, 1978; Watkins and others, 1978; Martin, 1980) and

beneath the upper slope. Basinward flow and intrusion of salt are thought to be caused by lateral loads exerted by the upslope sediment prism as well as the evolutionary history of thick salt deposits as they are deformed from salt sheets into walls, diapirs, and back into extensive salt sheets (Jackson and Talbot, 1986).

Secondary structural features within the basin fill were formed principally by gravity-driven tectonism. Most of the features occur near the paleoshelf margins and were created by tensional stresses and mobilization of salt and deep-water shale. The dominant features are large growth faults, salt diapirs, withdrawal basins, and local unconformities (figs. 4-9). Structures observed on seismic profiles are entirely within the sediment column and are above the basement; however, the mobile salt locally serves as a detachment surface (figs. 5-9). Salt deformation can be grouped into three broad zones, a shallow northern zone, a deep intermediate zone, and a shallow southern zone. Thick successions of middle and upper Miocene slope mudstones overlie salt in the northern part of the study area. These Miocene sediments progressively thin basinward reflecting the near surface position of salt beneath the late Miocene slope.

Most of the regionally extensive growth faults are aligned northeast-southwest (fig. 4). Less common alignments of fault traces are northwest-southeast and east-west. These alignments indicate that the principal direction of extension was to the south. The acute intersection of fault sets and variable orientations are related to local stress fields associated with the complex interplay of shelf margin deposition and salt mobilization. Some fault segments are oriented at high angles to the primary faults. They are known as cross faults or oblique transfer faults (Gibbs, 1984) because they accommodate different magnitudes of extension along the master fault.

In relatively old basins with variable subsidence histories, renewed movement along basement faults may affect the position and orientation of younger structures (Harding and Lowell, 1979). Primary alignments of structural features in the Plio-Pleistocene depocenter coincide remarkably well with orientations of an outer basement high and related transform fault systems proposed by Hall and others (1983). Close alignment of basement features (Pilger and Angelich, 1984) with relatively young syndepositional structures suggests that plate movement may continue to exert a strong influence on regional stress patterns. If shallow structures are partly related to crustal deformation, then the fracture patterns within the basement may be propagated into the sediment column by periodic minor adjustments along megashears and other zones of crustal weakness.

Principal Structural Features

Extensional Faults

Major growth faults disrupting Plio-Pleistocene strata form three classes: (1) regionally extensive expansion faults that roughly parallel the contemporaneous and former shelf margins, (2) subparallel counter-regional faults that correspond to and form basinward of the preceding class of faults but have the opposite displacement, and (3) highly arcuate faults (collapse faults) that circumscribe well defined salt-withdrawal basins. The term counter-regional fault is used because some up-to-the-basin faults are not antithetic to major synthetic faults; furthermore, most antithetic faults are secondary features that only cause minor stratigraphic displacement (figs. 5-9). Reactivation of older faults and several stages of faulting are common owing to the episodic movement of salt and migrating sites of diapirism.

Contemporaneous growth faults form where the shelf margin is convex-upward and laterally unconfined in a basinward direction. The over-steepened profile and low sediment strength create slope instabilities that promote detachment and downward rotation of large fault blocks. Slope failures range in scale from small rotational slump blocks and slides within a single, relatively thin depositional sequence to extremely large translation and rotation along regional growth faults. The middle slope, which has a concave-upward surface, may be composed of highly faulted or relatively unfaulted strata depending on the cohesiveness and stress state of the underlying beds. Theories explaining the mechanics of faulting, the geometries of growth faults, and their dependency on the competency of beds and rates of deposition were presented by Bruce (1973), Dailly (1976), and Crans and others (1980).

In map view, most fault traces are subparallel, semi-continuous, and have down-to-the-basin displacements (fig. 4) that cause abrupt increases in stratigraphic thickness. Some up-to-the-basin faults are small, graben-forming antithetic (stress relief) faults that terminate against the basinward side of the primary fault. Because of their small displacement, these antithetic faults are not shown on fig. 4. Counter-regional faults having large displacements commonly occur along the basinward margin of withdrawal synclines.

Three zones of counter-regional faults (fig. 4) mark major boundaries of salt mobilization. The oldest (Buliminella 1 and Globoquadrina altispira) counter-regional faults occur basinward of the upper Miocene shelf margin near the updip limit of shallow salt diapirs. Together the shallow salt diapirs and counter-regional faults mark the transition between deformed shale structures to the north and deformed salt structures to the south. The second zone of counter-regional faults occurs near the Trim A shelf margin. This fault zone also coincides with the transition between isolated salt diapirs of moderate size beneath the modern shelf and larger, more

continuous salt massifs beneath the slope. This fault zone contains the counter-regional fault system that is most continuous and has the greatest displacement. It is a product of simultaneous salt withdrawal and diapir growth. This fault system formed along the Angulogerina B-Hyalinea balthica upper slope during and after deposition of the Trimosina A (Trim A) sediments (fig. 4). Initially high-angle fault planes have been rotated to a low angle as a result of extension and salt reorganization. The third zone of counter-regional faults is located on the slope. The faults occur above nearly continuous salt massifs and reflect relatively recent salt mobilization influencing post-Trim A sediments. These faults intersect the seafloor and create escarpments having local relief of as much as 1000 ft (300 m).

Collapse faults tend to be local or subregional in their extent. They are younger toward the margin of the withdrawal syncline because support is progressively removed away from the syncline axis as salt is evacuated. This process can cause massive sediment failure around the margins of the withdrawal syncline and abrupt local thickening of sediment within the syncline.

Shale and Salt Diapirs

Basinward displacement of strata is initiated in the zone of extension and transferred downslope along glide planes coinciding with intrastratal discontinuities such as unconformities and bedding surfaces. According to deformation theory, extension near the shelf margin and translation across the upper slope (gravity gliding) must be balanced by compression farther down the slope. Along most active shelf margins, compression occurs on the middle to lower slope where shale ridges and small thrust faults originate. Compressional stresses extrude undercompacted, overpressured slope

deposits creating diapiric shale masses that, in turn, cause uplift and faulting of younger strata.

Large, incipient salt structures compose the greatest volume of sediment beneath the slope. The shapes, isolation, and vertical growth of these structures are best explained by differences in external and internal pressure around the salt mass and variability of shear strength of the surrounding country rock. These physical differences result from the complex interaction of sediment loading, regional extension, and salt movement. Salt domes beneath the slope typically penetrate to shallower depths than those beneath the shelf because the thin slope overburden composed of water-saturated mud has low shear strength. These conditions favor vertical dome growth. Deep-rooted piercement domes probably were mobilized as a result of Paleogene shelf margin progradation that loaded the thick salt wedge causing basinward flow and constructing linear ridges and broad pillows. These incipient salt structures subsequently were remobilized to form small discontinuous spines (Martin, 1980) that pierce and uplift the upper Miocene sediments but cause only minor sediment deformation around the domes.

The top of salt is recognized by broad, irregular, high-amplitude reflections or a change from coherent to incoherent reflections. The base of salt is uncertain because of the great depth (> 4.5 sec) and lack of seismic processing designed specifically to detect the base of salt or subsalt reflections.

Salt domes are the most common diapiric structure affecting Plio-Pleistocene strata. The spacing, size, and shape of these intrusive salt bodies changes in a basinward direction. Heights of intrusions with respect to the seafloor progressively increase basinward whereas absolute heights appear to increase and decrease in alternating bands. These broad paleoanticlines of salt are similar to those currently

intruding the distal apron of the Mississippi fan (Watkins and others, 1978). Beneath the modern slope of the western Garden Banks area (figs. 4 and 9), gradual and nearly continuous reorganization of salt is indicated by the general absence of faults between some salt structures.

Domes located on the updip flank or landward of the Plio-Pleistocene depocenter are narrow, nearly circular spines that are widely spaced, suggesting a mature stage of dome evolution (Woodbury and others, 1973). Rim synclines around some of these remnant diapirs indicate that necking, an internal salt reorganization mechanism, allowed the spines to maintain their shallow elevation as the sediment column aggraded. At the other extreme are allochthonous salt sheets on the lower slope, also referred to by various workers as salt sills, tongues, or wedges, that serve as the source for incipient dome growth. An intermediate stage of salt evolution is represented on the upper slope by large, nearly continuous massifs, which are separated by sediment filled sub-basins (fig. 9).

Shallow salt diapirs are absent throughout most of the West Cameron area (figs. 4-8). Residual salt mostly forms deep, low-relief structures. Thin salt sills are rare and occur at intermediate depths near the High Island-West Cameron boundary and near the center of the study area. The lack of shallow piercement is indicative of the mature stage of salt deformation. Large regional faults form where salt is absent or thin suggesting nearly complete extrusion downslope and laterally into salt diapirs. The discontinuity between sediments formerly separated by salt is known as a salt weld (Jackson and Cramez, 1989). Some remnants of salt or salt welds are preserved on the upthrown side of large faults near the intersection with the glide plane. Persistent sedimentation caused salt to migrate southward and westward into offshore Texas where shallow salt structures are more common (fig. 4).

Unconformities

Many unconformities within the Plio-Pleistocene strata can be observed on seismic lines, but they are limited in areal extent (figs. 5-9). Moreover, they are mostly related to syndepositional salt movement or slope failure and are typically restricted to uplifted areas.

The large sub-regional unconformity in the High Island area described by Morton and others (1991) extends into the westernmost part of the West Cameron area. This unconformity is a joint product of sediment mobilization and sea-level fluctuations. The "unconformity" is actually a composite slump surface or submarine pediment. Morton and others (1988) used the term submarine pediment to describe the broad disturbed zones of failed shelf margins. These non-deltaic entrenched features are wider than they are long and they form as a result of retrogressive slope failure and subsequent submarine erosion. The resulting embayment in the shelf margin focuses oceanic currents that initially excavate some of the slumped material. Some residual slump material is preserved above the detachment surface. Later the deepwater depression is filled with slope and shelf deposits. Thus, submarine pediments do not fit the standard morphological or genetic definition of a deep, relatively narrow incised valley-canyon system formed at the shelf margin by stream entrenchment during a lowering of sea level (Morton, in press).

Structural Styles

Structural deformation of Plio-Pleistocene strata in the northern part of the study area is generally simple (figs. 5-8). The salt is thin and deeply buried and structural features are widely-spaced faults, broad shale-cored anticlines, and narrow salt diapirs.

Most are late Miocene structures reactivated as mobile sediments reorganized in response to sediment loading. The oldest faults have northwest-southeast orientations that parallel the late Miocene shelf margin. Salt is overlain by a thick section of middle-upper Miocene and lower Pliocene slope mudstones. In turn, the updip Pliocene-Pleistocene sediments overlie relatively stable upper Miocene shelf and slope deposits. Stable depositional conditions are indicated by the lack of slumps and other mass transport features. The gradual basinward dip and slope stability suggest an interdeltic ramp that was supplied by across-shelf transport of fine-grained sediments. Counter-regional faults having minor displacements and deep salt diapirs are typical structures just basinward of the upper Miocene shelf margin (figs. 3-5). Displacement of youngest strata across the counter-regional faults is evidence of prolonged and persistent salt withdrawal (fig. 5). Farther basinward, fault spacing and stratigraphic displacement increase and progressively younger strata are deformed and structurally inverted. These structural and stratigraphic relationships were established as salt was extruded basinward and the top of salt served as a glide-plane surface.

In the eastern part of the study area, oldest growth faults are associated with zones of structural weakness inherited from the late Miocene to Glob a continental slope (figs. 4 and 6). Prolonged extension along the master fault (center of fig. 6) created rollover to the north while pronounced thinning and truncation of the Ang B section occurred to the south. This exceptionally long listric fault (fig. 6) has remained active since at least Glob a deposition; however, greatest growth and structural inversion occurred during the Glob a to Ang B depositional episodes. The fault originated on the basinward flank of a salt swell or ridge beneath the middle Pliocene (Bul 1 to Glob a) slope. The fault was repeatedly activated by deposition of

sand-rich submarine fans that are vertically stacked and serve as hydrocarbon reservoirs in East Cameron Block 299 and West Cameron Block 557 fields. The principal expansion fault displaced the pre-Glob a section as much as 8 mi (13 km) basinward (fig. 6). Counter-regional faults that formed on the landward side of the salt ridge also remained active as salt was evacuated from the ridge.

Structural features near the middle of the study area (fig. 7) are similar to those illustrated on the previous sections with the exception that counter-regional faults of Miocene age did not form. The oldest map unit (Rob E to Bul 1) records progradation of lowstand wedges and shelf-edge deltas over deformed upper Miocene and lower Pliocene deep-water shale. These regressive depositional events were accompanied by progressive basinward faulting in a stairstep pattern near the Glob a paleomargin. Faulting of slope deposits was related to deep salt mobilization that accompanied rapid deposition and progradation of Lent 1 sediments on the former slope. Nearby production in the West Cameron Block 450 field is from outer shelf and upper slope sandstones of the Lent 1 interval. The major growth-faults in the mid-dip position were most active during Ang B progradation. This family of faults traps hydrocarbons in Ang B and Hyal b sandstones that produce from fields in West Cameron Blocks 540, 563, and 587. Farther basinward, salt reorganization attendant with Hyal b deposition caused structural inversion of the pre-Ang B section and stratigraphic convergence within the Hyal b section (fig. 7). Stratigraphic thinning over the salt ridge was accompanied by abrupt thickening in the withdrawal basin where salt was evacuated to maintain the elevation of adjacent domes. Evacuation of salt from the adjacent slope created new accommodation space that was filled by a thick succession of Ang B sediments. Contemporaneous progradation of shelf-edge deltas and deposition of outer shelf and upper slope sandstones and mudstones created large

regional and counter-regional faults and rollover within the graben complex. The flank of this rollover structure serves as the trap for gas produced from Hyal b sandstones in the nearby West Cameron Block 630 field (fig. 7).

Shallow piercement salt structures are most common in the northern and western parts of the study area (figs. 4 and 8). Most of the shallow diapirs are narrow spines that have remained active as salt continued to migrate into the spines. Faults created by extension within the peripheral withdrawal syncline typically have minor displacements and stopped growing after Ang B deposition. The highest concentration of hydrocarbons is associated with numerous closely-spaced growth-faults that intersect the undulating surface of a salt platform (fig. 8). No single fault has dominated probably because the area was not the site of a major depoaxis. The top of salt, which was near the seafloor during Bul 1 and Glob a deposition, gradually subsided and only minor volumes of salt migrated into nearby structures. Consequently, basinward extension of the strata was also gradual. Basinward of the residual salt platform, growth faults disrupt the stratal continuity and form hydrocarbon traps in nearby West Cameron Block 612 and 633 fields (not shown on cross section). These young structures are connected with the Trimosina regional and counter-regional faults and intervening withdrawal syncline (fig. 8). Growth on the faults and adjacent salt structures occurred mainly in response to post Trim A deposition. Unlike their counterparts to the east, these faults cause only limited displacement of the oldest (pre-Lent 1) strata.

Large, irregular steep-walled salt stocks surrounded by faults are characteristic structures beneath the slope in the northern Garden Banks area (fig. 9). The faults are commonly concentrated near the stock although some faults occur within the adjacent withdrawal basins. In general, salt structure spacing, amplitude, and depth all

decrease basinward (fig. 9). Also, strata onlapping and overlying salt are younger basinward. The salt morphologies and stratal relationships are all evidence of progressively younger phases of salt deformation toward the center of the basin. Most of these faults and salt stocks have undergone late movement and some structural features are expressed by substantial relief on the seafloor.

Timing of Structural Movement

Five structural subregions are identified on the basis of ages of principal deformation (fig. 4). Inferred boundaries of the subregions parallel the northeast-southwest structural grain. As expected, ages of the structural features progressively decrease basinward, reflecting systematic outbuilding of the continental platform and attendant deformation near the contemporaneous shelf margin. The oldest structures are associated with the upper Miocene to Glob a shelf margins, whereas the youngest structures are related to Trim A and post-Trim A shelf margins. Exceptions to this systematic order of deformation are caused by reactivation of older faults and domes as well as creation of younger stress fields in older sediments.

Many of the faults and domes have had long, relatively continuous growth histories whereas some structures experienced moderately long periods of dormancy between periods of movement. Refaulted faults and faults folded or pierced by salt are preferentially located along the Bul 1 and Ang B expansion fault zones (figs. 4 and 6). The Bul 1 faults were mostly reactivated and penetrated during Lent 1 time whereas Hyal b salt movement was responsible for fault deformation along the Ang B trend. Few of the refaulted faults trap hydrocarbons probably because potential seals were disrupted and hydrocarbons, if present, leaked to the surface.

DEPOSITIONAL SYSTEMS, SYSTEMS TRACTS, AND GENETIC SEQUENCES

Depositional Systems

Depositional systems are three-dimensional assemblages of genetically related sedimentary facies (Fisher and McGowen, 1967). They include the deposits of common coastal plain and nearshore environments such as rivers, deltas, and barrier-strandplains as well as deeper water environments such as shelves, slopes, and abyssal plains. Most of these clastic depositional systems were present along the western Louisiana continental margin at some time during the Plio-Pleistocene with the exception of sand-rich barrier-strandplains. The rapid, high amplitude fluctuations in sea level prevented extensive reworking of nearshore facies and this precluded the preservation of thick barrier-strandplain deposits (Morton and Galloway, in press). This report emphasizes the shelf-edge delta systems and slope systems because they were the principal loci of sand deposition throughout the Plio-Pleistocene and their shifting positions ultimately controlled the distribution of hydrocarbon reservoirs.

Shelf-edge Delta Systems

The shelf-edge delta model (Winker and Edwards, 1983) is largely based on late Pleistocene and modern delta systems of the northwestern Gulf of Mexico. Both high resolution sparker and CDP seismic profiles display late Pleistocene depositional sequences, especially the Wisconsinan shelf-edge deltas that prograded onto the slope and filled intraslope basins (Lehner, 1969; Suter and Berryhill, 1985; Berryhill, 1987).

These constructional events occurred principally during falling stages of eustatic sea level and subsequent lowstands.

The modern highstand Mississippi shelf-edge delta has been examined in detail by Coleman and others (1983). They described the surficial landslides, large-scale slumps, and other deformation features that form as a result of gravitational instability along the oversteepened delta front. Other surficial features include carbonate reefs that grow on topographic highs in response to recent movement of shallow piercement salt domes.

High sedimentation rates and steep slopes associated with shelf-edge deltas create slope instabilities. The rapidly deposited sediments contain abnormally high water volumes and biogenic gases. These fluids create high pore pressures and decrease sediment shear strength that together may cause slope failure. Slope instability occurs at three different scales. Small-scale surface creep, slumps, and gullies are below the resolution of conventional seismic profiles. These features, which are tens of feet thick, are contained within the clinoform facies and contribute to progradation of the shelf margin (Coleman and others, 1983). An intermediate scale of sediment deformation involves large slope failure whereby blocks of sediment slide downslope and bedding is either preserved or distorted. This type of intraformational slumping encompasses a few hundred feet of sediment and occurs above a detachment surface that merges with bedding planes downslope. The largest scale of deformation includes deep-seated normal faults that grow in response to sediment loading at the shelf margin. These faults have throws of several hundred to a thousand feet and basinward displacements as great as several miles.

At the scale appropriate for basin analysis, the shelf-edge delta model is typified by thousands of feet of sediments, large-scale growth faults, preferential preservation of outer shelf and upper slope deposits, and an overall upward-coarsening log pattern representing relatively systematic basinward progradation. The positions of shelf-edge deltas are controlled by sediment supply and they can be either highstand or lowstand features. Thus, they are not always synonymous with the shelf-margin systems tracts of Posamentier and others (1988), which are lowstand features.

Slope Systems

The second primary depositional model used to interpret Plio-Pleistocene strata represents an aggradational slope system that has been greatly modified by syndepositional deformation. The contemporaneous tectonic influence creates active faults, salt diapirs, and withdrawal basins that control the patterns of deposition by forming preferred pathways of sediment transport within the topographic lows. An approximate depositional model for an aggrading slope system can be constructed by examining sedimentary characteristics of the Mississippi fan complex and those of the late Quaternary intraslope basins of the northern Gulf of Mexico.

Deposition of deep-water sediments and their relationship to glacio-eustatic cycles remains controversial. At least three different process-response models have been proposed to explain deposition of submarine fans on slopes of passive continental margins. Each of these submarine fan models can be supported by seismic evidence from the western Gulf Coast Basin and each is probably responsible for some deposition of Plio-Pleistocene deep-water sediments.

The most widely publicized slope system model explains deep-sea fan deposition as a result of river entrenchment near the shelf margin (Haq and others, 1987, Posamentier and others, 1988). The coarse clastics composing the fans are eroded from or by-passed across the shelf during falling sea level and lowstand phases of a eustatic cycle (Mitchum and others, 1977). An alternative glacio-eustatic explanation is that submarine fans are deposited by sediment slumped from the shelf margin during an initial rapid rise in sea level. The key to this depositional model is the high-volume discharge of dense glacial meltwaters that cause dramatic increases in coarse clastics transported by the principal rivers (Perlmutter, 1985; Steffens, 1986). A third model describes canyon formation and submarine fan deposition during rising sea level and highstand conditions when the interdeltic or non-deltic shelf margin is starved (Brown and Fisher, 1977). Canyons can be initiated and grow during rising phases and highstands in sea level by retrogressive failure and associated slumping of the shelf margin (Coleman and others, 1983). Initial canyon excavation is augmented by focusing of marine currents that become density currents as they flow down the canyon axis (Farre and others, 1983).

Mud-rich submarine fans of the western Gulf Coast Basin are typically elongate sediment lenses having their longest axes parallel to paleoslope. These submarine fans are supplied by canyons cut into the shelf margin that act as point sources. Principal elements of the submarine fan model are the canyon, upper fan, middle fan, and lower fan (Bouma and others, 1985). Most canyons form near the shelf-slope break and retreat landward as a result of headward erosion, downcutting, and slumping along the canyon walls. Locations of fan lobes are controlled by position of the canyon and by relief of the seafloor including topographic highs formed by older fans.

Characteristics of upper fans include a large channel and levee system that funnel sediment downslope. Channel-levee systems located at the apex of each fan are deep enough to confine deposition of coarse clastics, but shallow enough so that the upper part of the turbidity flow containing fine-grained suspended sediments is unconfined. Middle fans, which constitute the thickest parts of fans, are aggradational features composed of channel, levee, and overbank deposits. Much of the lower fan is deposited by unconfined flow discharged by shallow distributary channels that bifurcate and become indistinct near the fan terminus. Aggradational lower-fan deposits are crossed by several abandoned channels, but normally only one channel was active at any given time. Lower fan deposits may contain as much as 50 percent sand preserved as thin turbidite beds. They are generally devoid of planktonic forams, and benthic forams are commonly resedimented shallow-water species originally deposited on the inner or middle shelf (Woodbury and others, 1978).

Concepts of fan morphology, facies architecture, and slope processes derived from the Mississippi fan complex (Bouma and others, 1985) are extremely valuable for understanding Plio-Pleistocene slope deposits; however, their application to the Louisiana shelf and upper slope is somewhat limited. For example, the best documented middle and lower parts of the Mississippi fan are so large and their deposits so thick that the fan is not greatly influenced by diapirs. In contrast, Pliocene turbidites in southwestern offshore Louisiana, deposited as small submarine fans or in intraslope basins, were directly controlled by the surficial expression of diapirs on the contemporaneous upper slope. These Pliocene turbidites were deposited in a series of small, lowstand wedges that coalesced to form broad sandy aprons parallel to the shelf edge. Only a few narrow, lowstand submarine fans prograded down slope onto the basin floor. Furthermore, the coarsest Pliocene submarine channel

and fan deposits are composed of fine to very fine sand rather than coarse sand and gravel as reported for the youngest channel system of the Mississippi fan (Bouma and others, 1985).

Intraslope basins are another important component of the depositional model for Plio-Pleistocene slope deposits. Bouma (1982) recognized three classes of intraslope basins that he described as (1) blocked submarine canyons, (2) closed interdomal depressions, and (3) small collapse basins over structural crests. These local collapse structures over domes are common salt-dissolution features, but they are not significant for purposes of regional mapping.

Turbidity currents capable of transporting coarse clastics great distances down the slope are generally oriented nearly normal to the shelf edge. This is because the flow is gravity induced and this orientation produces the steepest downslope gradient. Diapirs protruding into the water column can create orographic effects that accelerate and deflect the flow causing locally diverse flow directions and increasing capacities of currents transporting coarse detritus through intraslope basins.

In the northwestern Gulf of Mexico near the outer shelf, bottom currents that are not turbidity currents generally flow to the northeast in response to wind forcing (Cochrane and Kelly, 1986) and occasional intrusion of the Loop current (Minerals Management Service, 1986). It is likely that flow directions were similar during the Plio-Pleistocene, considering the configuration of the Gulf of Mexico. Time-averaged velocities of near-bottom currents are low, but maximum instantaneous velocities can be as high as 2 ft/sec in water depths of 200 to 300 ft (Rezak and others, 1985). Except during storms, these prevailing non-turbidity bottom currents are relatively weak and are capable of transporting only fine-grained suspended sediments.

Depositional Systems Tracts

Depositional systems tracts were originally defined as contemporaneous depositional systems that are genetically linked (Brown and Fisher, 1977). Recently the concept of systems tracts has been applied to erosional and depositional process-related facies associated with lowstand, transgressive, and highstand phases of a eustatic sea-level cycle (Haq and others, 1987; Posamentier and others, 1988). According to the eustatic model, when the rate of fall in sea level is greater than the rate of subsidence at the shoreline break, the shelf is at least partly exposed and rivers incise valleys. This occurs in response to lowered base level and increased stream gradients. Large volumes of potentially coarse sediment eroded from the shelf are deposited on the slope and basin floor forming lowstand submarine fans (lowstand systems tract). As the rate of sea-level fall declines, channels aggrade and trap the coarse-grained sediments so that only fine-grained deposits reach the upper slope and fill the topographic lows created by the slump deposits. When relative sea level gradually begins to rise, deposition is largely confined to shelf-margin deltas and younger submarine fans (lowstand progradational wedges) deposited between the shelf edge and the basin-floor (lowstand) submarine fan. Consequently, basin-floor fan construction slows and turbidites are generally confined to the channel axes (Kastens and Shor, 1985). Together the basin-floor fan and lowstand progradational wedge principally aggrade the slope. If sediment supply is adequate and the lowstand phase is sufficiently long, the lowstand wedge may prograde over the fan deposits in response to maximum regression.

In contrast to deposition during a rapid fall and lowstand of relative sea level, a rise in sea level causes an abrupt landward shift in deposition (transgressive systems tract). Coarse sediments are trapped near the shoreline creating sediment starvation on

the shelf and slope and deposition of a marine condensed section. In deep water, only hemipelagic and pelagic mud is deposited as drapes over the fan surfaces. During the final stages of rising sea level and highstand (highstand systems tract), large delta systems prograde toward the shelf edge over the transgressive deposits while mud continues to accumulate on the slope. The highstand systems tracts are primarily responsible for progradation of the shelf margin.

As currently used, sea level systems tracts do not connote the types of depositional systems that were active when a particular stratigraphic sequence formed. They merely connote the inferred phase of a sea level cycle at the time of deposition. In this report, terms describing both depositional systems and systems tracts are used because (1) interpretation of Plio-Pleistocene strata in the context of eustatic cycles is appropriate, and (2) inclusion of both sets of descriptors conveys more information than either does alone.

In general there is good agreement between the coastal onlap curve of Beard and others (1982) and Haq and others (1987) and observed depositional cycles associated with the principal Plio-Pleistocene fluvial-deltaic systems (fig. 1). Minor differences between predicted and observed coastal onlap relationships are observed as local shelf-margin failure and gravity resedimentation that has the appearance of lowstand deposits, but are not shown on the Exxon sea-level curve (Haq and others, 1987). Other discrepancies are related to continuous chart revisions and the repeated inclusion of more fluctuations in the eustatic curve. Major discrepancies between observed and predicted stratal relationships are the thick Cristillaria S (lower Ang B) and Hyal b onlap wedges of slope sediments, which according to the Exxon curve were both deposited during rising or highstand phases of sea level rather than during falling phases of sea level.

Sequence Boundaries and Offshore Sequences

For more than four decades the petroleum industry has successfully used extinction horizons and other paleontological marker beds for subsurface correlation and mapping (Curtis and Picou, 1978). The extinction horizons commonly coincide with marine condensed sections and surfaces of maximum flooding, which are defined by faunal increases and low-sedimentation rates (van Wagoner and others, 1988; Loutit and others, 1988). These regionally correlative flooding surfaces form the basis for subdividing rocks into quasi-chronostratigraphic units known as depositional complexes (Frazier, 1974) or genetic sequences (Galloway, 1989). Genetic sequences are bounded by flooding surfaces (transgressive systems tracts) that are products of relative rises in sea level (Galloway, 1989). In contrast, stratigraphic sequences are bounded by unconformities and their correlative conformities (lowstand systems tracts) that are produced by falls in sea level (Vail and others, 1977). Thus, boundaries dividing genetic sequences and those dividing stratigraphic sequences are out of phase with respect to eustatic sea level cycles.

In this study, the post-Miocene section is divided into eight genetic sequences using biostratigraphic markers and their associated transgressive marine shales as sequence boundaries (figs. 1 and 2). The oldest genetic sequence encompasses lower to middle Pliocene strata (Robulus E to Buliminella 1) representing a period of about 1.5 Ma when muddy shelf and slope sediments slowly accumulated near the continental margin. The remaining seven sequences represent variable periods of time that generally decrease in duration with decreasing age (fig. 1). Buliminella 1 (Bul 1) to Globoquadrina altispira (Glob a) lasted about 900,000 yrs; Glob a to Lenticulina 1 (Lent 1) lasted about 600,000 yrs; Lent 1 to Angulogerina B (Ang B) lasted about 700,000 yrs. Ang B to Hyalinea balthica (Hyal b) lasted about 500,000 yrs. Hyal b to

Trimosina A (Trim A) lasted about 350,000 yrs. Trim A to Globorotalia flexuosa (Glob flex) lasted about 500,000 yrs. and post-Glob flex (Wisconsinan and Holocene) lasted about 150,000 yrs.

Onshore Formations

Onshore Plio-Pleistocene sediments composing the lower coastal plain of Louisiana are preserved as four formations (Williana, Bentley, Montgomery, and Prairie). These terrace-forming outcrops have been named, correlated, and subdivided principally using morphologic criteria such as elevation, slope, degree of dissection, and soil type (Fisk, 1939; Russell, 1940; Fisk and McFarlan, 1955; Bernard and LeBlanc, 1965). Morphostratigraphic analysis of late Quaternary deposits by these and other workers demonstrates that each formation is wedge-shaped, was deposited during a sea-level highstand, unconformably overlies and onlaps an older formation, and has a well-developed paleosol on its upper surface.

Youngest Pleistocene terrace deposits in Louisiana are known as the Prairie Formation, which is equivalent to the Beaumont Formation in Texas (Bernard and LeBlanc, 1965). The Prairie Formation represents fluvial, deltaic, and marginal marine deposits that retain much of their original depositional morphology. Geomorphic features commonly observed on aerial photographs include scroll bars, abandoned channels, and accretion ridges. The Prairie Formation is composed mostly of clay interbedded with fine-grained sand of variable thickness. Thickest sand deposits are associated with fluvial channels of the upper delta plain. Prairie Formation mudstones exposed near the coast contain brackish water fauna typical of estuaries and interdistributary bays.

Some early workers concluded that tectonic deformation in the source area controlled the systematic vertical changes in grain size observed in the Plio-Pleistocene coastal plain terraces. Other workers, however, recognized that glacio-eustatic sea-level fluctuations were responsible for the depositional cycles (Fisk, 1939; 1944).

Correlation of onshore Plio-Pleistocene formations with specific interglacial stages has been largely abandoned because (1) the number of climatic events and corresponding relative sea-level cycles greatly exceeds the number of named formations, (2) the coastal plain deposits have not been accurately dated, and (3) the onshore depositional record is incomplete. The latter condition is a result of erosional truncation and coastal onlap that preserves units in the subsurface that are not represented in outcrop.

Recently, McFarlan and LeRoy (1988) correlated the coastal plain outcrop units with thick genetic sequences mapped beneath the Louisiana continental shelf. Their work and the work of others show that the outcrop units are mainly minor progradational and aggradational deposits that accumulated during regional transgressions and maximum highstands of sea level, whereas the continental margin sediments were deposited mainly during lowstands of sea level.

PLIO-PLEISTOCENE STRATIGRAPHIC FRAMEWORK

Principal depositional systems and systems tracts for each of the Plio-Pleistocene genetic sequences were interpreted by integrating all available geological, paleontological and geophysical information. The primary types of data include vertical patterns of electric logs, biostratigraphic tops and paleoecological zones, net and percent sandstone maps, and seismic profiles. Comparing geologic maps and cross sections reveals

sediment transport pathways, which aids in the prediction of lithologies in areas of sparse or no well control. Such a comparison also explains the differences in paleogeographic reconstruction that result from independent mapping of systems tracts on the basis of seismic facies patterns and well data. Depositional systems maps constructed primarily on the basis of lithological and paleontological criteria tend to emphasize the most basinward platform construction associated with the youngest and shallowest progradational event before the ensuing transgression. In contrast, seismic facies maps emphasize the underlying deeper water sediments because these sediments commonly represent the thickest part of the genetic sequence.

Most of the principal genetic sequences of this study are so thick that they are composed of several depositional cycles, termed parasequence sets (van Wagoner and others, 1988). These parasequence sets can be observed on seismic profiles and identified from well logs (Pls. 1-3).

Mapping Depositional Systems and Shelf Margins

Log facies patterns typical of most of the Plio-Pleistocene sand-rich depositional systems are presented in figure 10. Diverse erosional and depositional processes can produce similar electric log patterns; therefore, depositional environments represented by these log facies patterns are difficult to interpret without other evidence. However, when maps of log facies patterns are combined with paleobathymetry, seismic facies, and regional geologic setting, they provide a useful tool for predicting lithologies and interpreting depositional systems.

Pattern A (fig. 10), which represents an onlap slope apron or submarine channel-fan complex, exhibits either a progradational or an erosional base and at least an upward thinning of sandstone beds if not an actual upward fining in grain size. This pattern is typical of some mid-dip and down-dip sandstone successions (wells 5 and 22, Pl. 1; wells 2-6; Pl. 2; and wells 1, 9, 11, and 17, Pl. 3). Pattern B typifies upward-coarsening distal delta-front and shelf sandstones deposited near the subsiding shelf margin. The basal progradational sequences in most wells commonly illustrate this pattern (Pls. 1-3). Pattern C represents progradational and aggradational nearshore sandstones such as distributary-mouth bars and gravity resedimented delta fronts. These are typical patterns in most wells (Pls. 1-3). Medium to thick sandstone packets with abrupt erosional bases (pattern D) characterize aggradational nearshore and coastal plain deposits associated with initial lowstands and rising phases of sea level. Examples are seen in the Ang B, Hyal b, and Trim A intervals in most wells (Pls. 1-3), and they are commonly associated with discontinuous, variable-amplitude seismic reflections.

Mixed blocky and upward-fining or upward-coarsening log patterns (pattern E) typically are associated with fluvial or delta-plain deposits representing channel and floodplain or crevasse splay environments respectively. These aggradational patterns can occur updip in any of the stratigraphic intervals (wells 3 and 4, Pl. 1; wells 1 and 2, Pl. 2). Pattern F is characterized by a thick, relatively sand-rich lower unit overlain by thin alternating sandstones and mudstones that grade upward into marine shales. This retrogradational facies architecture, which is commonly associated with a relative rise in sea-level, is illustrated by the youngest sandstones in the Hyal b and Trim A sequences (wells 5-8, Pl. 1; wells 7-11, Pl. 2; and wells 1-4, Pl. 3).

Recognition of paleomargins on the basis of physiographic slope or paleobathymetry is complicated when sea level fluctuations are extreme. If sea level falls below the former shelf margin, shallow-water neritic sediments (ecozones 2 and 3) are then deposited directly on the former slope. Under these conditions the seismically mapped highstand shelf edge will be landward of the lowstand outer neritic-upper bathyal (ecozone 3 and 4) transition. Conversely, if sea level rises substantially above the former shelf margin, deep-water "slope" sediments (ecozone 4) are deposited on the relict lowstand shelf landward of the geomorphic break in slope. An additional complication arises when relatively shallow-water fauna are locally transported from the shoreface and inner shelf into deep water by slope failure (creep, slump, turbidity currents). In vertical sequences of well cuttings this re-sedimentation has the appearance of an abrupt basinward shift in coastal sedimentation that might be misinterpreted as a rapid lowering of sea level.

Characteristics of Plio-Pleistocene Genetic Sequences

Pre-Robulus E (not mapped)

In the southern West Cameron area, middle and upper Miocene sediments are composed of mudstones with thin interbedded siltstones (well 1, PI. 1; well 4, PI. 2) that were deposited on the slope and basin-floor as turbidites and hemipelagic mud drapes. These deep-water deposits (ecozones 5 and 6) are several thousand feet thick and blanket the thin, remnant layer of salt. This stratigraphic relationship indicates that much of the salt migrated from the area as a result of shelf-margin progradation and loading of salt beneath the slope during the middle and late Miocene depositional episodes.

Miocene strata in the study area are recorded as high amplitude, continuous reflections, which suggest relatively uniform sedimentation on a shelf/slope ramp. These reflection patterns are not indicative of submarine channels and fans, slumps, or other high-energy turbidite facies that might contain thick beds of well-sorted sand. The Miocene strata were not subdivided and mapped in the study area because geophysical logs and seismic interpretations indicate that they are composed entirely of mudstones and do not contain reservoir-quality sandstones.

Robulus E to Buliminella 1 (Unit 1)

The Robulus E - Buliminella 1 genetic sequence (unit 1) is a wedge of coarse clastic detritus that thins westward and basinward. In the eastern part of the study area the sequence is composed of at least four parasequence sets (well 1, Pl. 3) that together constitute an upward-shoaling vertical succession. The oldest parasequence set is about 600 ft thick. It consists of thin interbedded sandstones and mudstones (serrate log pattern) that exhibit upward-fining and upward-thinning vertical profiles. These aggradational sandstones, which pinch out to the west, were deposited in a lower slope environment (ecozone 5). The lower slope sandstones grade upward into at least 600 ft of aggradational slope mudstones (ecozone 4-5) that comprise the second parasequence set. Above the slope mudstones are thin progradational sandstones having irregular to upward-coarsening log responses. The isolated sandstones are 20-50 ft thick and are interbedded with mudstones of comparable or greater thicknesses. The youngest parasequence set consists of a few blocky or upward-coarsening sandstones 100-200 ft thick that were deposited in an upper slope environment (ecozone 4). These slope sandstones also pinch out to the west and basinward into slope mudstones (ecozone 5).

In the western part of the West Cameron area, unit 1 represents initial progradation of coarse clastics over upper Miocene deepwater mudstones. This part of the sequence is characterized by extremely thin upward-coarsening sandstones separated by thicker mudstones (wells 1 and 3, Pl. 1). These interbedded sandstones and mudstones were deposited in inner to outer neritic environments (ecozones 2 and 3).

Net sandstone thickness of unit 1 is commonly 300 to 700 ft (fig. 11), except in the western part of the study area where net sandstone thickness is generally less than 200 ft. Sandstone abundance in unit 1 is controlled by contemporaneous deformation and location of the principal depositional systems. The highest concentrations of sandstone occur in small withdrawal synclines, which are former intraslope basins located between salt structures (compare figs. 4, 11, and 12). The greatest abundance of sandstone occurs where all the sand-rich parasequence sets are present. Sandstone constitutes less than 30 percent of the genetic sequence (fig. 12) because mudstone interbeds and mud-rich parasequence sets are common.

Seismic facies patterns of lower and middle Pliocene sediments (Rob E-Bul 1) are highly variable. They typically show a basinward change from variable amplitude, parallel reflections in updip areas to discontinuous, wavy-to-hummocky reflections in downdip positions. The sand-rich part of the sequence is entirely within the zone of continuous reflections. These seismic facies patterns indicate gradual accumulation of turbidites and hemipelagic muds on the slope rather than rapid accumulation as a result of mass transport processes. The zone of distorted seismic reflections occurs far basinward of the inferred shelf margin. Unit 1 is thin in the High Island East and western West Cameron areas where it was partly removed by large-scale failure of the shelf-margin and excavation during subsequent phases of lowered sea level (Morton and others, 1990).

The late Miocene-early Pliocene shelf margin of maximum progradation is poorly defined because it was altered in response to changes in relative sea level. First the paleomargin subsided and deepened. Mud accumulated on the outer shelf and upper slope, but sediment supply to the shoreline break was less than subsidence and the shoreline retreated.

Because these modifications tend to obscure the muddy late Miocene shelf margin, its approximate position is identified on the basis of an increase in regional dip of upper Miocene strata, increased number of faults, and increased fault displacement of Miocene beds. Upper Miocene sediments are buried progressively deeper to the east where the Plio-Pleistocene regional depocenter was located (compare Pls. 1 and 3).

Depositional systems of unit 1 were a sand-rich slope apron supplied by a relatively small shelf-edge delta system (fig. 13) that maintained a similar position during two separate eustatic cycles. The basal upward-fining slope apron (ecozone 5) is interpreted to be deposits of a lowstand systems tract. The Bul 1 slope apron in the West Cameron area is restricted to a zone within 12 mi (20 km) of the shelf margin (fig. 13). The thick succession of slope mudstones (ecozones 4 and 5) represent transgressive and highstand systems tract deposits whereas the overlying thin upward-coarsening slope sandstones (ecozone 4) were probably deposited by a progradational shelf-edge delta system (second lowstand systems tract) and its subsequent transgressive and highstand systems tracts.

The delta system consisted of both proximal and distal components. The western (distal) delta flank is composed of thin upward-coarsening outer shelf sandstones (ecozone 3) representing the second highstand systems tract. These distal deltaic deposits grade into a low-gradient mud-rich ramp supported by upper Miocene mudstones deposited mainly by lowstand and highstand systems tracts.

Only a few fields produce hydrocarbons from unit 1 (fig. 13). The reservoirs are typically restricted to either the slope apron (downdip) or to proximal deltaic deposits (updip). Most of the hydrocarbons appear to be associated with the youngest sand-rich highstand systems tract deposits.

Buliminella 1 to Globoquadrina altispira (Unit 2)

Facies architecture of unit 2 is highly variable because of the unstable shelf-margin setting, sea level fluctuations, and contemporaneous growth structures. As a result of complex sedimentation patterns, the electric log responses, sand body thickness, and lateral continuity of unit 2 sandstones are also highly variable. Three major episodes of sandstone deposition, hereafter referred to as basal, middle, and upper subunits, are recognized from well log patterns.

The basal subunit is penetrated only by wells in middip and downdip positions (well 5, PI. 1; well 6, PI. 2; and well 2, PI 3). It consists of aggradational sandstone beds ranging in thickness from 10 to 100 ft (3 to 30 m) and displaying mixed blocky, serrate, upward-coarsening, and upward-fining log patterns. The amalgamated beds form a sandstone package that is 500 to 700 ft (150 to 210 m) thick. Faunal assemblages associated with the sandstones are characteristic of the upper slope (ecozone 3.5-4) whereas the encasing mudstones were deposited on the middle slope (ecozone 4.5). The apparent upward shoaling is either the result of a lower sea level, middle slope resedimentation of outer shelf and upper slope deposits, or both. Chaotic seismic reflections in the basal part of unit 2 confirm that mass transport processes were responsible for at least some downslope movement of the sandy sediments.

The middle and upper subunits have similar sandstone thicknesses and log facies patterns. Both are about 400 to 500 ft (120 to 150 m) thick and both consist of amalgamated thin, upward-coarsening and blocky sandstones that are 5 to 50 ft (1.5 to 15 m) thick. Typical logs showing this progradational style of deposition are seen in wells 1-5 on plate 1. The only significant difference between the two subunits is that the upper subunit was deposited in slightly shallower water. Available paleoecological data indicate that the middle subunit was deposited on the outer shelf and upper slope (ecozone 3.5-4) whereas the upper subunit was deposited on the outer shelf (ecozone 3-3.5). Updip wells encounter the middle and upper depositional cycles, but the basal unit is absent. In updip positions, the middle and upper upward-coarsening cycles overly lower Pliocene and upper Miocene slope and abyssal plain mudstones (wells 1-4, Pl. 1).

Two styles of cyclic deposition are commonly repeated in unit 2. Either sandstones are distributed throughout the genetic sequence or sandstone thickness varies predictably with stratigraphic position. Those wells encountering the second style of deposition commonly exhibit thickest and best developed sandstones at the sequence base and thin, poorly developed sandstones near the sequence top or vice versa.

Sandstones of unit 2 are widely distributed, but individual sand bodies are discontinuous. Furthermore, sandstone abundance is highly variable in both strike and dip directions (figs. 14 and 15). Most wells penetrating depositional axes encounter from 100 to 300 ft (30 to 90 m) of sandstone, and a few wells penetrate more than 500 ft (150 m) of sandstone where all three sand-rich parasequence sets are present (fig. 14).

The principal sand axes are greatly influenced by syndepositional growth faults and diapirs having substantial relief on the paleocontinental slope. The northwest-southeast orientation of sandstone abundance (figs. 14 and 15) is controlled primarily

by sets of subregional growth faults (figs. 4) oriented parallel to the early Pliocene shelf margin (Bul 1, fig. 3). The most landward thick was created by salt reorganization and formation of a counter-regional fault (figs. 4 and 5). The southernmost sandstone depocenter is located within a local graben formed by a down-to-the-basin fault and associated antithetic faults. The intervening zone of low sandstone abundance represents a positive paleotectonic element that subsided more slowly than the adjacent withdrawal synclines. This positive structural feature is not salt cored but rather is composed of a thick succession of upper Miocene and lower Pliocene deepwater mudstones (well 3, Pl. 2).

Syn depositional sea-floor irregularities diverted slumps and turbidites preventing or minimizing the deposition of shelf and slope sandstones around salt structures. The diapirs created downcurrent shadow zones causing local thinning and shale out of some potential sandstone reservoirs. Sandstone concentrations in unit 2 are generally low and mostly range from 5 to 20 percent with some local deposits containing as much as 25 percent sandstone (fig. 15). These low sandstone concentrations reflect the moderately thick mudstones below and above the sandstone packages as well as numerous mudstones interbedded with the thin irregular sandstones.

Stratigraphic characteristics of the slope sandstones in unit 2 appear to be similar to those of the lowstand submarine fans of the adjacent High Island area (Morton and others, 1991). However, those slope and basin floor fans are highly elongate and extend more than 100 mi (160 km) basinward of the shelf edge. The basinward extent of the Glob altispira sandstones in the West Cameron South Addition area is poorly defined because few wells are drilled below 12,000 ft (3,600 m) where the submarine fan system is commonly encountered. On the sandstone abundance maps (figs. 14 and 15), the sand-rich submarine fan system is shown as being detached

from the progradational upward-coarsening sandstones of the lowstand wedge. Sandy facies of the submarine fan may cover a larger area than is shown and extend updip beneath the sand-rich part of the lowstand wedge.

The inferred zone of sand bypass and apparent predominance of unit 2 mudstone in the West Cameron South Addition Area (figs. 14 and 15) is also largely an artifact of drilling. Most wells penetrate structural highs that were also contemporaneous bathymetric highs; consequently, reservoir quality sandstones may be concentrated off-structure in intraslope basins. In the High Island area, contemporaneous slope deposits contain as much as 500 ft (150 m) of net sandstone just above salt (Morton and others, 1991).

Seismic facies patterns of unit 2 can be grouped into three zones. The most landward zone consists of a broad area of variable-amplitude, continuous reflections. Basinward dipping clinoforms are not well developed in unit 2 and are restricted to updip areas (fig. 16). Where present, clinoforms occur near the top or middle of the unit (fig. 7) and downlap onto the basal chaotic reflections. Clinoforms are poorly developed possibly because (1) gradients of depositional surfaces near the paleomargin were extremely low or (2) the clinoforms are obscured by syn- and post-depositional deformation.

Alternating high- and low-amplitude, parallel continuous reflections are typical seismic facies patterns of unit 2 especially in updip areas and even in the zone expanded by growth faults. These patterns typically grade basinward into low-amplitude, discontinuous, hummocky to wavy patterns with local slump features. The top of unit 2 commonly coincides with high-amplitude, parallel and continuous seismic reflections, whereas the base is poorly defined on seismic profiles.

The Bul 1 to Glob a genetic sequence (unit 2) represents an overall upward-shoaling succession. The sequence is composed of three distinct depositional cycles. This tripartite depositional pattern is in contrast to published sea-level curves that indicate one complete eustatic cycle (fig. 1, Haq and others, 1987; Beard and others, 1982) or two lowstands separated by a highstand. The paleogeographic setting was one of a delta-flank shelf margin that received a minor supply of coarse sediment. The low-gradient delta-flank ramp of unit 2 was adjacent to an entrenched system located mainly in the High Island area (Morton and others, 1991). The basal sandstones of each depositional cycle represent initial rapid deposition of coarse sediments onto the slope (ecozone 3.5 and 4) by gravity resedimentation in conjunction with a lowstand in sea level. Construction of this lowstand wedge was followed by a landward shift in coastal onlap and deposition of mud on the slope (ecozone 4 and 4.5) by transgressive and highstand systems tracts. This change in sedimentation style accompanied deposition of a shelf-edge delta (ecozone 2 and 3) (fig. 16). The repetitive pattern of both upward-fining and upward-coarsening sandstones records slope aggradation (lowstand and transgressive systems tracts) and subsequent deltaic progradation across the continental platform (highstand systems tract).

The slope apron sandstones are generally restricted to a zone within 25 mi (40 km) of the shelf margin (fig. 16), whereas sand-rich submarine fan deposits are encountered as much as 60 mi (96 km) basinward of the paleoshelf margin. Glob a slope sandstones are thicker and more numerous to the west away from the area where Bul 1 sandstones were deposited (compare figs. 11 and 14). To the west in offshore Texas, slope sandstones of comparable age extend more than 100 mi (160 km) basinward of the shelf margin. This significantly greater basinward transport was

the result of a broad entrenched system that focused turbidity currents down the slope where sand was concentrated within leveed channels and elongate submarine fans (Morton and others, 1991).

Hydrocarbons in unit 2 are generally confined to resedimented sandstones deposited in a lowstand systems tract (fig. 16; well 5, Pl. 2; wells 1 and 2, Pl. 3). Most of the fields are located near the paleomargin on the upper slope and along contiguous depositional axes (figs. 5 and 16). Hydrocarbon reservoirs in unit 2 range in depth from about 5,000 ft to nearly 9,500 ft (1,500 to 2,900 m) with depths generally increasing eastward and basinward. Currently deepest known accumulation in unit 2 is in West Cameron Block 459, which is located in a graben complex.

Globoquadrina altispira to Lenticulina 1 (Unit 3)

Unit 3 can be broadly divided into two lithofacies groups on the basis of vertical well-log profiles. The most common and widely distributed lithofacies group consists of amalgamated sandstones that are 10 to 100 ft (3 to 30 m) thick and have upward-coarsening or blocky log responses. This lithofacies group (Pls. 1-3) is normally restricted to the most updip area. The upward-coarsening sandstones overlie either (1) the second sandstone type displaying mixed serrate and upward-fining patterns or, more commonly, (2) at least 500 ft (150 m) of marine shale. These basal progradational deltaic and shelf sandstones were deposited in relatively shallow water (ecozone 3 to ecozone 1) and near the shoreline.

The second lithofacies group consists of thin, highly irregular sandstones interbedded with thin mudstones. These sandbodies exhibit a mixture of serrate, upward-coarsening, and upward-fining log patterns (wells 7-13, Pl. 3). Composite

aggradational sandstone packages are as much as 1,000 ft (305 m) thick, but most are about 300 ft (90 m) thick. The amalgamated sandstones occur above the marine shale containing the Glob a extinction horizon. They also commonly grade upward and basinward into marine mudstones. The irregular sandstone distribution was influenced by local failure of the shelf margin (fig. 8) and excavation of a submarine canyon (fig. 6) that supplied the lower Lent 1 submarine fans.

Unit 3 sandstones are irregularly distributed and discontinuous over most of the study area. The general pattern of sandstone distribution reveals alternating dip-oriented (north-south) bands of high- and low-sandstone concentration (figs. 17 and 18). The distribution of Lent 1 (unit 3) sandstone abundance is nearly inversely related to that of the Glob a genetic sequence (unit 2) (figs. 14 and 17). In unit 3, net sandstone thicknesses are commonly 100 to 500 ft (30 to 150 m); thicknesses greater than 500 ft (150 m) delineate depositional axes (fig. 17). Anomalous east-west trends in unit 3 lithofacies maps are related to syndepositional growth faults as well as salt and shale diapirs (compare figs. 4, 17, and 18). The depositionally controlled north-south axis and structurally controlled east-west axis result in a complex lithofacies distribution.

Sandstone concentrations in unit 3 are generally less than 25 percent (fig. 18). Local sandstone concentrations greater than 25 percent coincide with the primary depositional axes, whereas areas of low sandstone concentration coincide with structural highs, indicating syndepositional salt and shale reorganization.

Seismic reflection patterns within unit 3 are complex, but they generally display systematic changes in a basinward direction. High-amplitude or alternating high- and low-amplitude, parallel continuous reflections characterize the most landward zone of

seismic patterns. This zone also contains low-angle clinoforms that downlap onto the lower sequence boundary of unit 3 (fig. 7). Clinoforms are best developed where the genetic sequence is relatively thin and composed of less than 300 ft (90 m) of net sandstone (compare figs. 17 and 19). Low-amplitude, discontinuous and chaotic reflections are typical seismic patterns of unit 3 basinward of the Lentic 1 shelf margin and associated expansion fault zone (fig. 4).

Integrating well log and seismic facies patterns with paleoecological zones indicates that unit 3 is an upward-shoaling sequence. The most updip upward-coarsening log patterns are evidence of transgressive and highstand systems tract deposits, whereas moderately-elongate slope sandstones near the base of unit 3 are lowstand submarine fans and slope aprons that grade laterally and basinward into slope shale (fig. 19). Concentration of sandstones at the base or in the middle of unit 3 indicates that the sand transport pathways on the slope were maintained or repeatedly reoccupied. High rates of subsidence and sedimentation are indicated by beds of alternating sand and shale preserved in the lowstand fan (mixed serrate and upward-fining lithofacies) basinward of the paleoshelf margin. These slope sandstones are thicker than correlative slope sandstones in offshore Texas (Morton and others, 1991), but they do not extend as far basinward of the paleomargin.

Strata above the lowstand slope deposits are predominantly progradational mudstones and sandstones associated with a river-dominated delta system (lowstand wedge) that gradually advanced the continental platform about 25 mi (40 km) basinward of the Glob a shelf margin (fig. 19). Coastal-plain, deltaic, and shelf sandstones composing the lowstand progradational wedge exhibit both elongate and lobate patterns. They also grade basinward into slope shale. In the southern part of

the West Cameron area, the downdip limit of these lowstand sandstones is not well defined because no wells have penetrated this interval south of the Trimosina fault zone (figs. 4 and 19).

Hydrocarbon production from unit 3 sandstones is not constrained by sedimentary facies (fig. 19). Nevertheless, no significant accumulation of hydrocarbons in unit 3 is located landward of the Glob a shelf margin and the downdip limit of Lent 1 suppression. The most updip Lent 1 fields produce from shorezone and deltaic deposits of a highstand systems tract (fig. 8) whereas the largest fields produce from slumped delta-front or slope sandstones of the lowstand submarine fan facies (fig. 6; well 7, Pl. 1; well 11, Pl. 3).

Lenticulina 1 to Angulogerina B (Unit 4)

The facies architecture of unit 4 varies systematically depending on geographic and stratigraphic position within the depositional systems tracts. In updip areas sandstones are blocky, aggradational, areally extensive and 200 to 300 ft (60 to 90 m) thick. These sandstone packages are separated by beds of marine shale or interbedded thin sandstones and mudstones approximately 50 ft (15 m) thick. Examples of this predominantly nearshore and inner shelf (ecozone 2) depositional pattern are illustrated by wells 1-4 on plate 1. Wells in middip positions encounter thin upward-coarsening sandstones and interbedded marine shales that were deposited in outer shelf environments (ecozone 3-3.5). In a few centrally located middip wells, thick marine mudstones contain isolated, thin (200 ft, 60 m) upward-coarsening sandstones at the base and top of the sequence (well 12, Pl. 2). This sand-starved areas (figs. 20 and 21) is related to contemporaneous uplift on the subregional Ang B

expansion fault zone and possibly a mud-filled entrenched system. Seismic evidence that could resolve this difference in interpretation is inconclusive because of poor data quality.

The thickness and log facies patterns of unit 4 change abruptly basinward of the major Ang B expansion faults (fig. 4). The expanded Ang B section typically is comprised of three sand-rich parasequence sets (wells 17 and 18, Pl. 1; wells 13 and 14, Pl. 2). The oldest parasequence set is bounded by the Lent 1 and Cristellaria S (Robulus 64) extinction horizons. The younger two parasequence sets occur between the Cristellaria S and Ang B extinction horizons. Each parasequence set is 1,000 to 2,000 ft (305 to 610 m) thick and composed of vertically stacked, mixed upward-coarsening and upward-fining sandstones. Some paleontological reports indicate that the oldest parasequence set is in the upper Lent 1 (unit 3) genetic sequence. However, detailed well log and seismic interpretations demonstrate that this basal parasequence set is slightly younger than unit 3 and the paleontological discrepancies are probably the result of faunal reworking. The lower two sand-rich parasequence sets are relatively uniform in thickness along depositional strike whereas the upper mud-rich parasequence set is wedge shaped and pinches out to the east and to the west.

The most downdip sandstone facies of unit 4 are uncertain because the Ang B fauna is not reported for wells in the southern West Cameron South Addition and Garden Banks areas (fig. 22). Apparently the basinward limit of faunal occurrence is related to the upper slope depositional environment that precluded growth of the benthic foram population in water depths greater than about 450 ft. Where the Ang B fauna is present, the sequence is characterized by variable log responses that include mixed upward-fining and upward-coarsening patterns (wells 19-23, Pl. 2). The parasequence sets exhibiting these characteristics are composed of isolated and

discontinuous sandstones 15 to 30 ft (4.5 to 9 m) thick that appear to be randomly distributed throughout the genetic sequence. These thin sandstones are encased in thick slope mudstones, which were deposited in ecozones 4 and 5.

Sandstone distribution in unit 4 is closely related to penecontemporaneous deformation as well as local failure of the shelf margin (fig. 7). Sandstone is thin or absent near salt diapirs, shale ridges, and horsts. Net-sandstone thicknesses are typically greater than 500 ft (150 m) and locally exceed 2,000 ft (600 m) (fig. 20). Deepwater shale appears to be the predominant lithology in the southern West Cameron and adjacent western Garden Banks areas. Sandstone concentrations in unit 4 are between 5 and 68 percent (fig. 21) and concentrations greater than 30-60 percent delineate the depositional axes. Because the Ang B stratigraphic marker is uncertain in downdip wells, a map of net sandstone that includes both the Ang B and Hyal b sequences was prepared to emphasize the thickness and distribution of post-Lent 1 sand-rich depositional systems in the Garden Banks area (fig. 23).

Clinoform reflections are present in unit 4 (fig. 6) but are not well developed (fig. 22) probably because of the high sandstone concentration and syndepositional deformation. Seismic profiles show that fluvial incision is common in updip areas. Chaotic seismic reflection patterns are persistent basinward of the subregional Ang B fault zone. This zone of disturbed sediments coincides with the three parasequence sets.

Depositional systems analysis of unit 4 (fig. 22) indicates that the updip blocky sandstones were deposited on the stable platform as deltaic and other nearshore facies by transgressive and highstand systems tracts. In contrast, the thin, amalgamated upward-coarsening parasequence sets at the top of the sequence were deposited as distal-deltaic and outer-shelf facies also associated with transgressive and highstand

systems tracts. Depositional axes of the updip sandstones were largely inherited from the Lent 1 genetic sequence (figs. 19 and 22). Parasequence sets of unit 4 mainly exhibit mixed upward-fining and upward-coarsening vertical profiles immediately basinward of the Lent 1 fault zone and shelf margin. These aggradational and progradational deposits represent initial construction of the continental platform and subsequent upbuilding and outbuilding of the shelf margin by a lowstand progradational wedge and highstand shelf-edge delta system. Southward flowing coastal-plain rivers fed the large shelf-edge delta system that prograded about 20 to 25 mi (32 to 40 km) basinward of the Lent 1 shelf margin (fig. 22). The extremely thin, highly irregular downdip sandstones represent distal turbidites deposited on the adjacent lower slope. The Ang B slope sandstones were deposited immediately basinward of the Lent 1 slope sandstones (figs. 17 and 20).

The great influx of sediment deposited by the shelf-edge deltas initiated or reactivated regional growth faults and salt domes. These structures created additional accommodation space that trapped most of the coarse clastic detritus. As a result, unit 4 deposits are extremely thick near the paleomargin and rapidly thin downslope (fig. 20). Basinward transport of most coarse detritus was obstructed by fault blocks and diapirs near the contemporaneous shelf margin.

Unit 4 contains more hydrocarbon reservoirs (fig. 22) than any of the other genetic sequences; whether or not it also contains the largest volume of hydrocarbons compared to other Plio-Pleistocene sequences is unknown because reserve estimates are not differentiated for each reservoir in multiple reservoir fields. Some hydrocarbons in unit 4 are preferentially trapped in the Crist S lowstand progradational wedge (fig. 8), but most are contained in the slightly younger shelf margin delta sandstones (well

10, Pl. 1; well 13, Pl. 2). The reservoirs are resedimented delta-front deposits transported by mass movement as evidenced by chaotic seismic facies. Basinward pinchout of these lowstand deposits upthrown and structurally high on the Trim A fault zone (wells 12 and 13, Pl. 3) represent a possible basinward extension of this sequence. The most updip fields in unit 4 produce from shorezone sandstones deposited by transgressive and highstand systems tracts (fig. 7).

Angulogerina B to Hyaline balthica (Unit 5)

Four electric-log patterns describe the facies architecture of unit 5 depending on geographic location and depositional setting. The most updip wells encounter thin, aggradational interbedded sandstones and mudstones in the lower half of the sequence. These undifferentiated paralic or nonmarine deposits grade upward into shorezone deposits characterized by two massive blocky sandstones about 200 ft (60 m) thick separated by a shale interval about 20 ft (6 m) thick (wells 3 and 4, Pl. 2). Slightly farther downdip unit 5 is composed of several aggradational blocky sandstones that are each about 200 ft (60 m) thick (wells 6-8, Pl. 2). These sand-rich parasequence sets were deposited in middle neritic environments (ecozone 2). Middip wells typically encounter upward-coarsening sandstones that are vertically stacked in parasequence sets up to 300 ft (90 m) thick (wells 14-17, Pl. 2). This facies architecture is accompanied by a decrease in sandstone abundance because marine mudstones of comparable thickness separate the sandstones. These outer shelf sandstones (ecozone 3) thin basinward just updip of the Trimosina fault zone (fig. 8). Repeated collapse and excavation of the Hyal b shelf margin (figs. 5 and 8) promoted gravity resedimentation of the outer shelf sands.

Within and south of the Trimosina graben complex, unit 5 is composed of aggradational, mixed upward-coarsening and upward-fining parasequence sets that are 300 to 600 ft (90 to 180 m) thick (well 20, Pl. 1; wells 19-25, Pl. 2). The sands were originally deposited in shallow water (ecozones 2 and 3), but were subsequently redeposited in upper and middle slope environments (ecozones 4 and 5). Extensive re-sedimentation is revealed by the chaotic seismic facies as well as by the deep water mudstones that encompass the slope sandstones. The slope sandstones extend into the northern Garden Banks area, but their downdip limit has not been established because of the sparse number of exploration wells (fig. 24). Furthermore, net and percent sandstone values for unit 5 in the Garden Banks area are somewhat imprecise because the Ang B fauna is absent basinward of the Trimosina expansion zone (fig. 22).

Net-sandstone thicknesses of unit 5 are typically less than 700 ft (210 m). The principal depositional axes indicate southerly transport across the Louisiana shelf (figs. 24 and 25). Secondary east-west bands of higher net-sandstone thickness are related to movement of salt diapirs and growth faults near and landward of the Ang B shelf margin. Unit 5 sandstones thin over active salt-cored highs near the shelf margin and are mostly absent in contemporaneous slope deposits of the adjacent withdrawal synclines (fig. 24). Percent sandstone values for unit 5 range from less than 5 to more than 75 percent (fig. 25). This large range in sandstone concentration is due to facies changes as well as the influence of salt domes and growth faults.

The Hyal b collapsed shelf margin and entrenched system (figs. 5 and 26) was located between the contemporaneous salt-cored growth structures where the Hyal b and Ang B markers converge upthrown on major Trimosina faults. The convergence of the Ang B and Hyal b correlation markers over paleotopographic highs (figs. 5-7 and 26) explains why the second extinction horizon of Ang B coincides with the Hyal B

(unit 4) correlation marker in some wells. The paleotopographic highs caused substantial thinning of unit 5 and a concomitant increase in mudstone deposition. The thinning is observed in seismic reflections that commonly merge in the hanging wall near the fault plane (figs. 5-7). The convergence of mapping horizons records the reduced accommodation space that accompanied simultaneous uplift and lowering of base level. The timing and stratigraphic significance of structural deformation in unit 5 is similar to that in the adjacent High Island area (Morton and others, 1991).

The principal axes of sandstone deposition for unit 5 (fig. 26) are evidence of repeated and prolonged occupation of fluvial-deltaic systems. These rivers and deltas occupied areas that subsided at moderately high rates due to evacuation of salt while adjacent structurally positive areas were buttressed by salt diapirs and fault-bounded horsts. Low net sandstone values updip of the Trimosina fault zone (figs. 4 and 24) are related to erosion and/or nondeposition of Hyal b sediments.

Seismic facies of unit 5 can be broadly divided into two groups on the basis of reflection amplitude. High-amplitude, parallel, continuous reflections are persistent landward of the Trimosina fault zone, whereas low-amplitude, discontinuous or divergent reflections occur basinward of that zone. Clinofolds are absent from most of unit 5 (fig. 26) because the section that normally would contain these reflections is extremely thin or eroded. Where present, clinofolds downlap onto the contorted sediments of the collapsed shelf margin (fig. 5).

Depositional systems of unit 5 (fig. 26) are similar to those of the older stratigraphic units with two exceptions: (1) slope sandstones are limited in their lateral extent seaward of the shelf margin and (2) geological responses to fluctuations

in relative sea level and tectonic activity were more complicated. Growth of a salt swell into a salt ridge near the Ang B shelf margin elevated the Hyal b section. This uplift removed or prevented significant sandstone deposition except in the central part of the West Cameron South Addition area.

Slope sandstones of unit 5 basinward of the Trimosina fault zone were deposited near the shelf margin rather than on the slope or the basin floor. These thick sand-rich parasequence sets were deposited by lowstand shelf-edge deltas and later transported farther downslope by slumps and turbidity currents. Deposition occurred near a river mouth where growth faulting and a relative rise in sea level created additional accommodation space. Most of the updip and middip sandstones were deposited as transgressive and highstand systems tracts in delta plain, delta front, and shelf environments where subsidence rates were relatively low. The underlying stable platform, which was constructed during the Ang B (unit 4) regression, minimized the rates of subsidence. Accommodation space for these sediments was created mainly by a relative rise in sea level.

Most of unit 5 in the central part of the West Cameron South Addition area was transported downslope during excavation of a minor submarine canyon (fig. 5). The canyon was located just landward of the failed Ang B shelf margin (fig. 26). The youngest episode of slope failure and entrenchment occurred during a falling sea level and lowstand shortly before the Hyal b transgression. Associated lowstand deposits locally form a relatively thick wedge of sand-rich sediments. Basinward of the Trimosina fault zone, the last occurrence of Hyal b is commonly reported near the basal unconformity. This is because the Ang B-Hyal b section was removed by erosion. Excavation of the submarine canyon and associated deposition (fig. 5) contradict the coastal onlap curve of Haq and others (1987) and Beard and others

(1982). Both of those curves indicate only deposition by highstand systems tracts for the Ang B to Hyal b depositional episode.

Most of the hydrocarbon accumulations in unit 5 are located landward of the shelf margin (figs. 5, 7, and 26). The gas is trapped in the upper part of the highstand systems tract sandstones just below the regional Hyal b shale. This youngest sandstone succession exhibits an upward-fining facies architecture that documents coastal retrogradation that accompanied the Hyal b terminal transgression. The few downdip reservoirs (fig. 7; well 18, Pl. 2) are thin, amalgamated sandstones deposited on the outer shelf and upper slope by a shelf-edge delta system.

Hyalinea balthica to Trimosina A (Unit 6)

The facies architecture of unit 6 also varies depending on geographic location and stratigraphic position. In updip wells, the sequence is composed of alternating blocky sandstones and thin, interbedded sandstones and mudstones arranged in several parasequence sets approximately 200-300 ft (60-90 m) thick (wells 1-4, Pl. 1; wells 3-15, Pl. 2). The updip sand-rich parasequence sets commonly are sharp-based but in middip positions they grade into upward-coarsening, blocky, and upward-fining parasequence sets (wells 11-19, Pl. 1) reflecting progradation, aggradation, and retrogradation in relatively shallow water (ecozone 2). Stratigraphic thickness in updip and middip areas is relatively uniform because of slow subsidence and minor structural deformation. Despite the uniformity in stratigraphic thickness, sandbodies are discontinuous as a result of depositional processes in nonmarine and transitional environments.

Facies architecture of unit 6 is less systematic basinward of the Trimosina fault zone where mixed upward-coarsening and upward-fining parasequence sets are composed of amalgamated thin sandstones and interbedded mudstones. The sand-rich parasequence sets have a serrate log pattern and are as much as 700 ft thick (wells 19-23, Pl. 2; well 15, Pl. 3). Most of the sandstone in sequence 6 occurs in the lower two-thirds of the sequence. The upper third is characterized by upward-coarsening then upward-fining log patterns indicating progradation followed by retrogradation. Faunal assemblages associated with these parasequence sets indicate deposition in outer shelf and upper slope environments (ecozones 3 and 4). The upward-fining and upward-coarsening sandstones thin basinward where they are separated by thick intervals of slope mudstones (ecozones 4 and 5).

Net-sandstone thickness (fig. 27) and sandstone percent (fig. 28) of unit 6 define two separate trends. The northeast-southwest trend parallels the primary depositional axes, whereas the northwest-southeast trend reflects interaction of syndepositional faulting, subsidence and sediment supply. Alternating bands of thick and thin net sandstone are a response to downwarp and structural rotation near the master fault plane and stability or minor uplift over structures formed downdip near the youngest family of faults (fig. 5-8). Despite large net sandstone thicknesses in the expansion zone (fig. 27), percent sandstone values are low (fig. 28) because intercalated shales are also thick (wells 19-23, Pl. 2). Dip-oriented sandstone thicks of unit 6 are slightly offset compared with prominent depoxes of unit 5 (compare figs. 24 and 27). Except in the Garden Banks area, salt does not penetrate unit 6 because of its relatively young age and great thickness (figs. 27 and 28).

Sandstone abundance decreases near the Hyal b shelf margin, reflecting a basinward thinning of the interval above a former discontinuous salt ridge as well as a basinward decrease in sand deposited by the lowstand and transgressive systems

tracts. Steep contour gradients on net and percent sandstone maps (figs. 27 and 28) coincide with the lowstand progradational and aggradational sandstones.

The updip limit of thick lower Trim A sandstones is controlled by the Trimosina expansion fault zone, whereas the downdip limit of thick sandstones coincides with the counter-regional fault zone (figs. 4, 6, and 8) except where feeder channels pass into the western Garden Banks area. Lower Trim A sandbodies are probably channel-fill and shorezone deposits that aggraded during lowstand and rising phases of sea level. They were then transgressed and buried by a blanket of outer shelf and upper slope mud during the ensuing highstand.

Seismic reflections of updip strata of unit 6 have variable amplitudes and variable continuities; discontinuous erosional surfaces and small incised channels are also common. Middip seismic signatures are mostly high-amplitude, continuous and parallel reflections. These seismic patterns pass basinward into low-amplitude, parallel reflections that are either continuous or discontinuous. Hummocky to wavy reflection patterns of the lowstand wedge are generally restricted to the most basinward zone of low-amplitude reflections.

Low-angle clinoform reflections are common near the Hyal b shelf margin (fig. 29), which also coincides with the transition zone between discontinuous and continuous reflections. Clinoforms are absent in the eastern half of the study area where sandstone percent is high (compare figs. 28 and 29). In the middle of the study area, clinoforms in the basal part of unit 6 downlap onto the Hyal b shale (figs. 7 and 8). These progradational seismic facies occur basinward of the Hyal b clinoform zone and landward of the Trimosina fault zone (figs. 7 and 8).

Unit 6 is composed of several depositional systems (fig. 29). In updip and middip positions, it is composed of aggradational coastal plain facies. The sand-rich facies were deposited by fluvial-deltaic and barrier strandplain systems whereas the mud-rich facies were deposited by chenier plain or lagoon systems representing the transgressive and highstand systems tracts. In downdip positions the highstand and lowstand shelf-edge deltas and adjacent slope systems (fig. 29) prograded the Hyal b to Trim A continental margin from 6 to 20 mi (9.6 to 32 km) with distance decreasing away from the depocenter.

The Hyal b-Trim A stratigraphic interval (unit 6) is the youngest Plio-Pleistocene sequence of offshore southwestern Louisiana having substantial hydrocarbon reserves and exploration potential. Most of the gas reserves are limited to the southern half of the study area (fig. 29) where sandstone abundance is greatest. Most of the hydrocarbons are trapped at the top of thick sandstone parasequence sets deposited by shelf-edge delta systems near or basinward of the Hyal b shelf margin (fig. 6; wells 21 and 24, Pl. 2). Retrogradational sandstones deposited in response to the relative rise in sea level associated with the Trim A transgression are also important reservoirs. Other minor accumulations are related to vertical migration around salt domes and leakage from older reservoirs (fig. 7). The northeast-southwest trend of fields producing from unit 6 cuts across depositional grain and associated facies boundaries reflecting the dominant structural control on hydrocarbon distribution (fig. 29).

Trimosina A to Globorotalia flexuosa (Unit 7)

Unit 7 is the youngest hydrocarbon-producing sequence of thick shelf-margin deposits in the West Cameron South Addition area. Furthermore, it is the least deformed Plio-Pleistocene sequence with enough well control to map regional genetic

stratigraphy. Therefore, it serves as a good analog for some of the older Plio-Pleistocene sequences that were influenced by sea-level fluctuations and rapid subsidence.

Only some wells were logged through unit 7 because of its shallow depth. Those logs reveal that the balance among sediment supply, subsidence, and eustasy favored a dominantly mud-rich retrogradational and aggradational facies architecture (Pls. 1-3) compared to the progradational and aggradational architecture of underlying Trimosina A sediments (unit 6). Furthermore, the locus of thickest, most massive nearshore sandstone deposition shifted landward compared to unit 6. Typical electric log patterns for updip and middip wells indicate thin, upward-coarsening and upward-fining sandstones separated by mudstones of comparable or greater thickness (wells 11-18, Pl. 1; wells 11-18, Pl. 2; and wells 2-13, Pl. 3). A few updip well logs record sharp-based, blocky channel-fill sandstones as much as 150 ft (45 m) thick (well 5, Pl. 2; and well 1, Pl. 3).

Unit 7 abruptly thickens and both lithofacies and biofacies change dramatically basinward of the Trimosina fault zone. Within the Trimosina graben, unit 7 is composed of sand-rich parasequence sets (wells 19-22, Pl. 2) deposited in outer shelf and upper slope environments (ecozones 3.5 to 4). The sandstone parasequence sets generally range from 200 to 400 ft (60 to 120 m) thick. Basal sandstones are discontinuous in strike and dip directions, whereas the uppermost parasequence set is composed mostly of thin, upward-coarsening sandstones at the top of the sequence. The uppermost sandstones are relatively continuous over their limited area of deposition. These outer shelf and upper slope sandstones abruptly pass basinward into slope mudstones (ecozones 4 and 5).

Patterns of sandstone abundance and sandstone concentration for unit 7 (figs. 30 and 31) illustrate that the subregional depocenters were inherited from unit 6. Most of unit 7 contains less than 300 ft (90 m) of net sandstone and is composed of less than 30 percent sandstone. Sand concentration is low even within the graben complex where unit 7 is about 2,000 ft (610 m) thick. The downdip lobate sand-body geometry in the southern West Cameron area is an artifact of the Trimosina graben system. Secondary updip depositional axes represent the locus of fluvial-deltaic deposition on the relatively stable platform previously constructed by deltaic systems of units 5 and 6. Aggradation rates in the graben complex were exceptionally high as salt evacuation and a relative rise in sea level created accommodation space.

Seismic stratal patterns of unit 7 in updip positions are variable-amplitude, mostly wavy and discontinuous reflections with small cut-and-fill erosional features. Interconnected fluvial systems landward of the Trimosina fault zone are expressed as channels encompassing hummocky to wavy reflections. These irregular reflections disrupt the surrounding high-amplitude continuous reflections. These seismic facies pass basinward into variable-amplitude, parallel, continuous reflections located in mid-dip positions and updip of the Trimosina fault zone. Basinward of the Trimosina fault zone, seismic reflections are disorganized and chaotic. On seismic profiles, these chaotic zones are characterized by intraformational slumps and other syndepositional deformation features indicative of mass transport near the shelf margin. These zones of deformed strata typically occur near the top of the sequence and are underlain by conformable high-amplitude reflections or downlapping clinoform reflections. Slumping and mass transport processes were responsible for resedimentation of the upper third of the sequence, whereas the lower third is dominantly progradational.

Low- and high-angle clinoform reflections are prominent near the transition between the parallel and chaotic reflection patterns. The seismic facies transition coincides with the Trimosina fault zone, which continued to influence patterns of deposition. Clinoforms typically occur near the basal part of the sequence and downlap onto the Trim A transgressive shale. This type of progradational pattern is seen across the southern West Cameron South Addition area (fig. 32). Near the West Cameron-High Island boundary, clinoforms occur in the middle of unit 7 (fig. 8). In each of these settings the clinoforms grade basinward into discontinuous wavy reflections.

The lowstand and transgressive systems tracts of unit 7 are composed of coastal plain and nearshore lithofacies. The lithofacies include fluvial channel sandstones and associated floodbasin mudstones, platform deltaic sandstones, and prodelta mudstones containing middle and outer shelf (ecozone 2 and 3) faunal assemblages. These platform facies grade westward into delta-fringe and shelf sandstones and mudstones (fig. 32).

The thick succession of sediments in the Trimosina graben complex was deposited primarily in outer shelf and upper slope environments (ecozones 3 and 4) by a lowstand shelf-edge delta system. The Glob flex shelf margin remained in approximately the same position as the Trimosina A shelf margin except near the West Cameron-East Cameron boundary, where maximum deposition of coarse clastics advanced the continental platform about 6 mi (10 km) basinward (fig. 32).

Unit 7 offers only minor exploration potential for hydrocarbons. Sandstones associated with the lowstand deltas serve as the hydrocarbon reservoirs deposited near the paleoshelf margin (fig. 32; well 20, Pl. 2). Most of the gas in unit 7 was trapped within the Trimosina A graben complex. The hydrocarbon accumulations are aligned in a northeast-southwest trend that is oblique to the regional structural trend.

Post-Globorotalia flexuosa (Unit 8)

Sediments above the Globorotalia flexuosa correlation marker are generally less than 1,000 ft (300 m) thick. In the Trimosina graben complex as much as 2,000 ft (600 m) of Wisconsinan age sediments were deposited (fig. 8, Pls. 2). Late Quaternary sandstone trends and interpreted depositional systems were not mapped for unit 8 because too few electric logs record the near-surface sedimentary section. This shallow interval has been extensively studied by Suter and Berryhill (1985), Berryhill (1987), and Coleman and Roberts (1988) who used numerous high-resolution seismic profiles and engineering foundation borings to reconstruct the post-Sangamon depositional history of the Louisiana-Texas outer continental shelf.

Results of these investigations are applicable to the present study because they provide insight into the composite nature of shelf margin deposits and the influence of both major and minor fluctuations in relative sea level. Integration of lithologic descriptions and seismic profiles of unit 8 permits detailed mapping of meandering streams within entrenched valley systems, delta lobes, and related barrier island systems, as well as the types of sequence boundaries and internal stratal patterns that are commonly used to interpret multichannel seismic data.

SUMMARY OF DEPOSITIONAL AND STRUCTURAL HISTORY

Late Miocene and Early Pliocene (6.0 Ma - 3.7 Ma)

During the late Miocene (pre-Robulus E, fig. 1), widespread coastal regression initially advanced the continental platform in offshore southwestern Louisiana and southeastern Texas, but later the platform subsided and was flooded as sediment

supply diminished and relative sea level rose. In southwestern offshore Louisiana, primarily aggradational and retrogradational distal deltaic, outer shelf, and upper slope sandstones and mudstones were deposited.

The basinward extent of progradational clastic wedges were progressively shifted landward as the shoreline/shelf equilibrium entered a retrogradational phase (Morton and others, 1988). Mud-rich transgressive systems aggraded the continental slope and constructed a broad interdeltic ramp as evidenced by the thick succession of fine-grained upper Miocene-lower Pliocene sediments (wells 4 and 5, pl. 1) deposited in abyssal and lower slope environments (ecozones 6 and 5). The retrogradational phase of deposition culminated with the Robulus E regional transgression (5.5 Ma, fig. 1) and was followed by the aggradational phase of marine mud deposition lasted through the extinction of Textularia X (4.6 Ma, fig. 1)

Following the late Miocene and earliest Pliocene transgression and highstand in sea level, the principal drainage systems flowing into the Gulf of Mexico responded to a slight fall in sea level by rapidly prograding the shoreline and delivering coarse clastics to the contemporaneous outer shelf and upper slope. The axis of this deposition in Louisiana was located slightly west of the locus of late Miocene deposition (Woodbury and others, 1973). In the West Cameron area, the middle Pliocene Bul 1 interval (unit 1) contains thin, upward-coarsening sandstones of distal deltaic and shelf origin encased in thicker prodeltaic and shelf mudstones. These early Pliocene depocenters were supplied by shelf-edge deltas that constructed a slope apron of lowstand wedges and a delta platform near the paleo-shelf margin (fig. 13). The sand-rich deltaic systems passed westward and basinward into mud-rich shelf and slope systems, respectively.

The rising sea level phase of the early Pliocene depositional cycle culminated about 3.7 Ma in a widespread transgression containing the Buliminella 1 (Glob. nepenthes) extinction horizon (fig. 1). Water depths increased across the outer shelf and upper slope, but the relative rise in sea level was minor compared to existing water depths; therefore changes in faunal assemblages were insignificant.

Middle Pliocene (3.7 Ma - 2.8 Ma)

The middle Pliocene rapid influx of coarse terrigenous clastics (unit 2) also coincided with an abrupt fall in sea level about 3.0 Ma (Beard and others, 1982). This lowered base level exposed the continental shelf and caused entrenchment of fluvial systems within a submarine pediment in the adjacent High Island area (Morton and others, 1991). In the West Cameron area, sand deposition was restricted to the slope apron and submarine fans near the contemporaneous shelf margin (fig. 16).

Bathymetric highs controlled the pathways of sand transported downslope. Some emergent salt structures and fault escarpments trapped the coarse bedload of turbidity currents, whereas other bathymetric highs merely deflected the turbidity currents and focused them between growing structures, permitting deposition farther downslope. During the sea-level lowstand, slope systems delivered sand at least 30 mi (48 km) basinward of the paleo-shelf margin. The transport of coarse clastics to the slope diminished as the rate of falling sea level approached the rate of subsidence. Eventually a relative rise in sea level flooded most of the platform (transgressive systems tract) and caused retreat of the shoreline to a position similar to that during the early Pliocene transgression. At the same time, slope deposition terminated except for hemipelagic mud that was draped over the submarine fan deposits.

The marine condensed section associated with the middle Pliocene transgression contains the Glob a extinction horizon (2.8 Ma). The Glob a faunal assemblage is absent in updip wells because (1) it did not live in nearshore environments and (2) the Glob a highstand in sea level was not as high and therefore marine inundation was not as widespread as during the preceding Bul 1 (3.7 Ma) and following Lent 1 (2.2 Ma) highstands.

Late Pliocene (2.8 Ma - 2.2 Ma)

About 2.4 Ma (fig. 1) sea level abruptly fell to a position near or below the 3.0 Ma lowstand (Beard and others, 1982; Haq and others, 1987). This regressive event (unit 3) is seismically expressed updip as an erosional unconformity and downdip as clinoforms downlapping onto the Glob a condensed horizon (fig. 7). Sand transport pathways were mostly inherited from the previous (Glob a) slope apron system (figs. 14 and 17). The slope sands are thickest where rapid deposition along the unstable shelf margin remobilized salt and created additional accommodation space. This lowstand depositional event terminated when sea level stabilized. Continued subsidence resulted in a relative rise in sea level that reduced sand supply to the slope except for redistribution of slump deposits by turbidity currents near the shelf margin. Mud drapes buried the submarine fan deposits isolating them from the overlying progradational sandstones, which were deposited by multiple lobes of a shelf-edge delta system.

The relative rise in sea level that ended deposition of sequence 3 caused irregular landward retreat of the shoreline and an upward-deepening succession of marine mudstone deposited by outer-shelf and upper-slope systems. The marine condensed section associated with this transgression commonly contains the extinction horizon of either Lent 1 or Glob miocenica (2.2 Ma).

Early Pleistocene (2.2 Ma - 1.5 Ma)

The early Pleistocene depositional megacycle (unit 4) began about 1.7 Ma; however, the major influx of coarse clastic detritus was related to a fall in sea level about 1.6 Ma. Thick sandstone parasequence sets (fig. 20) constructed a lowstand wedge, which is located principally in the West Cameron South Addition area (fig. 22). This regressive depositional episode aggraded the slope and advanced the continental margin far beyond the maximum Lent 1 shelf edge. It also juxtaposed sand-rich nearshore deposits on thick slope mudstones of the Lent 1 transgressive and highstand systems tracts. The sandy lowstand wedge is generally thickest and best developed west of the Lent 1 submarine fans (figs. 17 and 20).

Rapid loading of salt structures on the upper slope caused simultaneous fault activation, dome growth, and development of withdrawal basins. Despite these potential sediment traps, a substantial volume of sand was transported downslope more than 60 mi (96 km) basinward of the shelf margin. At the end of this regressive episode (unit 4), maximum progradation of the shelf margin coincided with the discontinuous salt ridge complex that extends across the West Cameron South Addition area.

The early Pleistocene slope systems are preserved as sand-rich parasequence sets deposited by turbidity currents that originated near the contemporaneous shelf margin. Most of the deltaic sandstones are vertically stacked outer shelf deposits, indicating a balance between shelf margin subsidence and sediment supply. The regressive depositional phase was terminated by a relative rise in sea level about 1.5 Ma (Ang B transgression). This basinwide transgression caused a landward shift in the shoreline, deposition of outer-shelf mudstones over the deltaic deposits, and deposition of upper-slope mudstones on the adjacent ramp (transgressive systems tract).

Middle Pleistocene (1.5 Ma - 0.65 Ma)

After the regional Ang B transgression, moderately large delta systems prograded across the stable platform and beyond the paleoshelf margin leaving a record of upward-coarsening sandstone and mudstone parasequence sets (unit 5). Thicknesses of the delta deposits depended partly on water depth. Thick lowstand wedges formed in relatively deep water seaward of the Ang B shelf margin whereas thin deposits accumulated in relatively shallow water on the stable platform.

Faults and salt diapirs in the West Cameron depocenter were active during this depositional episode as demonstrated by substantial changes in stratigraphic thickness in isolated fault blocks between the salt ridge complex and the Ang B expansion fault zone (figs. 6 and 7). Reactivation and subsidence along faults and concomitant uplift or stability along a salt ridge near the High Island-West Cameron boundary captured much of the coarse sediment near the shelf margin and prevented significant basinward transport. However, farther to the east, sand was transported across the shelf-margin fault zone and far down the slope by a combination of slumping and shelf margin entrenchment.

The initial regressive event may have occurred during a highstand or it may have been a response to a slight lowering of sea level (fig. 1). In either case, a later lowering of base level (0.8 Ma) caused valley entrenchment in the West Cameron area and a basinward shift in deltaic sedimentation that resulted in deposition of thick outer shelf and upper slope sandstones on upper slope mudstones. At the same time, moderately thick sandstones aggraded the stable platform.

The subsequent relative rise in sea level terminated slope sandstone deposition and shifted the shoreline landward. A thin, but pervasive marine mudstone containing the Hyal b fauna accumulated over the former coastal plain during this brief transgression about 1.0 Ma (fig. 1).

Another major period of regression (unit 6) followed the Hyal b marine transgression. Two types of lithologic evidence suggest that this regressive episode was partly in response to a lowering of sea level. First, thick aggradational sandbodies having sharp erosional bases above the Hyal b marine shale are common throughout the updip area where the continental platform was slowly subsiding. Second, an extremely thick interval of outer shelf and upper slope sandstones was abruptly deposited by shelf-edge delta systems on the Ang B-Hyal b slope resulting in a basinward shift in coastal sedimentation. These lowstand depositional systems aggraded the slope and prograded the shelf margin. Faulting and salt diapirism also continued as rates of sedimentation rapidly increased.

Late Pleistocene (0.65 Ma - present)

The Trim A regional transgression about 0.65 Ma was followed by rapid outbuilding of the shoreline and reconstruction of the shelf margin near its Trim A position. The thick interval of vertically stacked, upward-coarsening cycles (unit 7) records the prolonged presence of small shelf-edge delta systems and their subjacent slope systems that deposited mud and some sand near the paleoshelf margin. This regressive event was aided by a fall in sea level that concentrated deposition on the former slope. As with the previous depositional cycle, much of the sand accumulated in the Trimosina graben system, but the fine-grained suspended sediment escaped the trap and was deposited as hemipelagic drapes on the adjacent slope.

During the falling sea level phase, discontinuous sandstone lenses were deposited above the Trim A marine shale wedge. As eustatic sea level stabilized with respect to subsidence, slope mudstones accumulated in advance of the prograding shelf-edge delta system. This delta system deposited the overlying thin upward-coarsening sandstones near the top of the sequence, which is capped by the Glob flex transgressive shale.

The youngest Quaternary parasequences were deposited after the Glob flex transgression (unit 8) in response to lowered sea level that exposed the continental shelf, caused valley incision, and initiated construction of lowstand wedges along the edge of the continental platform. These moderately thick lowstand wedges were deposited by shelf-edge deltas that prograded into relatively deep water and then began aggrading as the balance between subsidence and sediment supply attained near equilibrium conditions. Minor fluctuations in relative sea level and lobe switching caused repeated inundation and abandonment of delta lobes and their subsequent reoccupation.

Approximately 18 Ka, sea level began to rise as global temperatures warmed and glaciers melted. The rise in sea level was so rapid that the transgressive systems tract is represented by a marine erosional surface (ravinement surface) or a thin condensed section that still persists over much of the shelf. Although a highstand in sea level was reached about 5 Ka, highstand systems tracts have only formed at the Mississippi delta, the adjacent chenier plain, and at regressive barrier islands along the Texas coast where sediment supply was sufficient to prograde the shoreline (Morton and Galloway, in press).

HYDROCARBON GENERATION AND DISTRIBUTION

Plio-Pleistocene sediments along the outer continental shelf of the northern Gulf of Mexico produce large volumes of gas and condensate and some oil. Considering the entire trend, most of the Plio-Pleistocene production and recoverable reserves are located in offshore southwestern Louisiana. Although these young sediments have been buried to substantial depths, they are still relatively cool and diagenesis is not advanced (Milliken, 1985). Sandstone porosities and permeabilities are typically greater than 25 percent and hundreds of millidarcys, respectively, and reservoir quality primarily depends on the original pore properties and sandstone continuity inherited from the depositional environment.

This section reviews probable sources of the hydrocarbons, describes the geologic attributes of each hydrocarbon play in the West Cameron and western Garden Banks areas, summarizes the potential for undiscovered hydrocarbons in each play, and offers possible strategies for discovering the remaining reserves.

Source Rock Potential, Thermal Maturation, and Petroleum Migration

Available organic geochemical analyses indicate that all of the oil and most of the gas trapped in Plio-Pleistocene reservoirs originated much deeper in the basin. The hydrocarbons migrated to their present position as a result of cross-formational flow along deep-seated faults and around salt domes. Compelling evidence of vertical migration comes from integrated time and temperature indexes, which suggest that the producing sediments are thermally immature and therefore have not expelled oil and thermogenic gas (Dow, 1978; Huc and Hunt, 1980). The few available reports that

contain organic geochemical data for Plio-Pleistocene strata in the western Gulf Coast Basin demonstrate that the sediments contain ample quantities of organic matter, especially of the amorphous marine type that favors oil generation. Dow and Pearson (1975) analyzed the organic content of Plio-Pleistocene sediments in cores and cuttings of wells in the western Gulf of Mexico including some in the West Cameron and western Garden Banks area. They reported a progressive basinward increase in average weight percent organic carbon content ranging from 0.26 percent in inner neritic mudstones to 0.71 percent in mudstones deposited in abyssal environments. Samples from mid-shelf to abyssal depths all had average organic content exceeding 0.5 weight percent, which is considered a minimum value for petroleum generation.

Despite having adequate concentrations and favorable composition of organic material for hydrocarbon generation, the Plio-Pleistocene sediments of offshore Louisiana lack other important requirements necessary to convert the organic matter to hydrocarbons. Maturation profiles of Cenozoic sediments in Louisiana indicate that Plio-Pleistocene sediments would have to be deeper than 18,000 ft (5,500 m) and hotter than about 325° F in order to initiate in situ oil generation (Dow, 1978). Therefore, oil in Plio-Pleistocene reservoirs is inferred to have migrated from deeper source rocks. Additional evidence of vertical migration from great depths is the fact that produced oils are typically older than the reservoirs (Young and others, 1977).

Carbon isotope data from offshore Louisiana fields confirm that nonassociated gas trapped in Plio-Pleistocene reservoirs is a product of several processes (Rice, 1980; Nunn and Sassen, 1986). The shallow dry gas is of biogenic origin having been generated by microbial action during early stages of burial while the sediments were relatively cool. The isotopically heavier gas, a byproduct of generating liquid

hydrocarbons, was both physically separated during vertical migration and chemically fractionated by thermal distillation. At high temperatures, liquid hydrocarbons are thermally cracked to form gaseous hydrocarbons as strata subside and pass beneath the oil window.

Geochemical evidence suggests that slope mudstones of early Tertiary age (Eocene and older) are the most likely sources of thermogenic gas in Plio-Pleistocene reservoirs. However, deeply-buried Cretaceous carbonates beneath the salt are the most likely source of oil trapped beneath the upper slope (Nunn and Sassen, 1986; Dinkleman and Curry, 1988; Sasson, 1990; Thompson and others, 1990).

Spatial Distribution of Hydrocarbons

Plio-Pleistocene fields in the West Cameron and western Garden Banks areas (fig. 33) have produced more than 840 million barrels of oil equivalent (1 boe = 6 Mcf of gas) during the past 20 years. This volume of produced hydrocarbons indicates a moderately significant concentration of gas-prone fields in the western part of the Plio-Pleistocene trend.

Seismic and well log data were used to identify two types of combined structural and stratigraphic traps that account for most of the fields containing more than 25 million boe. Timing of salt movement is an important criteria for both types of traps. (1) The first type of trap includes the faulted crest and the basinward flank of large rollover anticlines. The rollover structures are associated with master listric faults that formed as a result of late salt movement. Nearly all the largest gas accumulations occur in this structural setting. (2) The second type of trap is associated with

relatively late salt dome growth which caused abrupt thinning of young sediments. Hydrocarbons are commonly trapped beneath the zone of stratigraphic convergence. Stratal convergence above the objective horizon indicates salt dome growth after development of a seal and focusing of migrating fluids into the resulting structural high.

Plio-Pleistocene sediments in the West Cameron and western Garden Banks area contain more than 1.1 billion boe in about 100 fields or local accumulations (fig. 33, Append.). Some fields contain more than 50 million boe (fig. 34, Append.) but most fields contain less than 10 million boe in recoverable reserves. The NRG Associates (1988) field-size data (fig. 34) follow a typical exponential decline curve, which indicates a finite limit in the number of large fields. The three largest Plio-Pleistocene fields (fields 59, 74, and 64, fig. 33) each contain between 102 and 150 million boe in recoverable reserves (Append.), and are anomalously large accumulations that represent the upper limit of expected field sizes (fig. 34).

The largest Plio-Pleistocene fields in the West Cameron-western Garden Banks area produce from Trim A (unit 6), Hyal b (unit 5), and Ang B (unit 4) reservoirs. The few fields containing nearly 100 million boe in multiple vertically stacked pay zones are preferentially located between the Trimosina regional and counter-regional faults (figs. 4 and 33). Many fields, including most of the larger fields, are associated with structures having some late fault movement. Only a few small fields are located near the intersection of several large faults or re faulted faults probably because of disruption in reservoir continuity and possible leakage along fault planes.

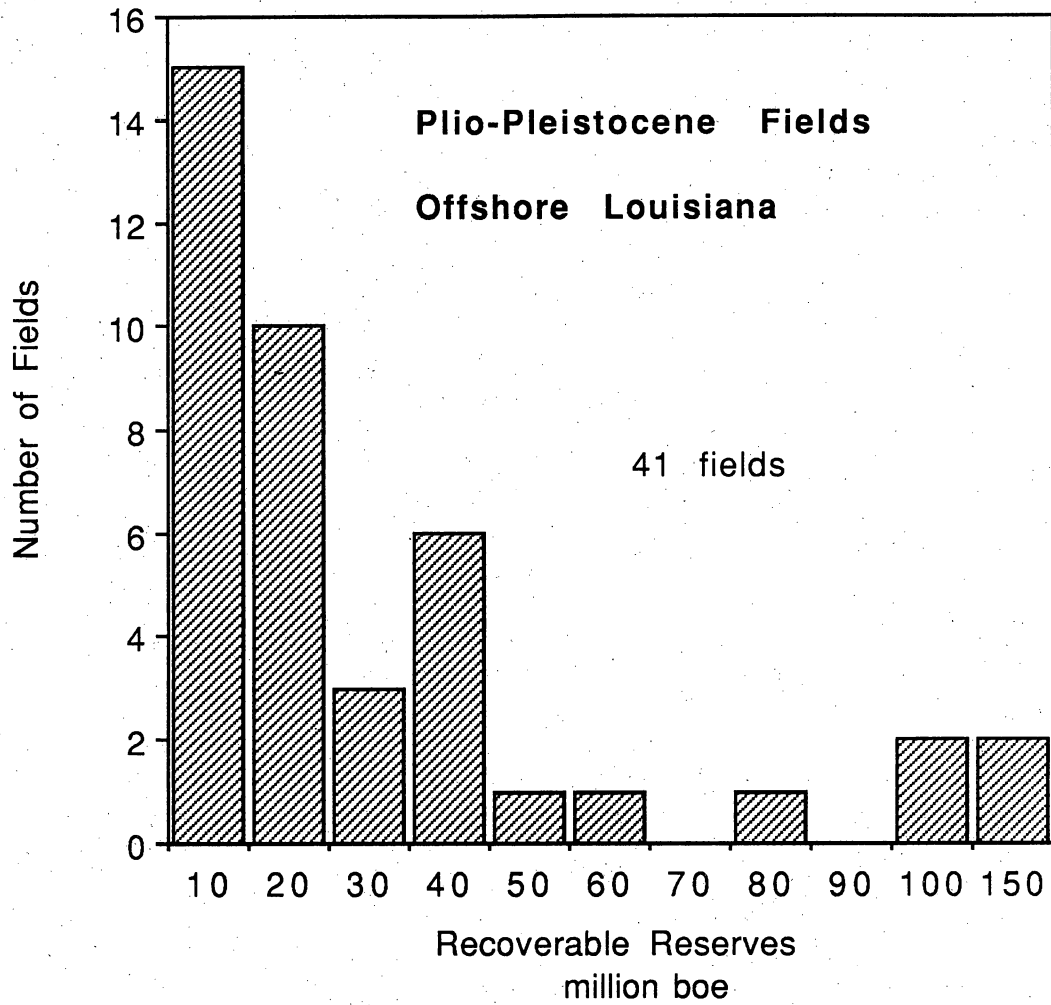


Figure 34. Sizes of known Plio-Pleistocene oil and gas fields in the West Cameron and western Garden Banks areas. Field sizes were determined on the basis of recoverable reserves reported by NRG Associates (1988).

Delineation of Hydrocarbon Plays

Hydrocarbon play analysis is a technique used to organize and to subdivide multiple diverse occurrences of petroleum within a regional trend or within a basin. As defined by White (1980), a hydrocarbon play is a group of oil or gas fields having similar geological characteristics including source rocks, reservoir facies, trapping mechanism, and hydrocarbon composition.

Producing fields or other significant petroleum accumulations within Pliocene Pleistocene strata were compiled for the West Cameron and western Garden Banks area using public as well as proprietary sources of information. The hydrocarbon indicators included: (1) zones of high resistivity directly observed on well logs; (2) depths of perforated intervals recorded on completion cards (subsequently corrected for deviation); (3) depths of producing reservoirs reported by NRG Associates (1988); and (4) symbols on well location maps. The NRG Associates data base also includes the ratio of total liquids versus gas, which indicates the predominant type or mix of hydrocarbons produced from each field.

Reservoirs within fields were assigned to stratigraphic intervals and interpreted facies on the basis of depths observed on electric logs, depths projected into adjacent structural cross sections, or depths projected into adjacent interpreted seismic lines. The hydrocarbon compositions, stratigraphic assignments, and reservoir facies designations were integrated with the structural framework to delineate the plays. Results of the play analysis, which includes fields of all sizes, are summarized in figure 33 and in table 1.

After establishing play boundaries, cumulative production and recoverable reserves were aggregated for fields within each play (fig. 35, Append.). The production and reserve estimates were derived from a proprietary computerized data base provided by

Table 1. Summary of geologic characteristics and exploration potential of Plio-Pleistocene hydrocarbon plays in the West Cameron and western Garden Banks areas.

Play 1

Hydrocarbon Type(s): Gas and minor amounts of oil.

Defining Attribute(s): Progradational middle to late Pliocene shelf margin

Reservoir Facies: Progradational and aggradational outer shelf and upper slope sandstones (Bul 1 and Glob a).

Structural Style: Shallow salt spines, shale ridges, and counter-regional growth faults formed by salt migration near the upper Miocene continental margin.

Trapping Mechanisms: Dip reversal and truncation associated with growth faults and shale ridges as well as stratigraphic pinch-out.

Possible Hydrocarbon Source(s): Subjacent lower Tertiary slope mudstones.

Exploration Maturity: Moderately mature to immature

Frontiers: Some untested minor stratigraphic traps. Possible extension of Bul 1 sandstones.

Limitations:

1. Basinward limit of sandstone deposition.
2. Discontinuity of slope sandstones.
3. Possible low recovery efficiency.

Play 2

Hydrocarbon Type(s): Gas.

Defining Attribute(s): Progradational continental margins of upper Pliocene and lower Pleistocene delta systems and subjacent slopes.

Reservoir Facies: Progradational and aggradational delta-front and slope sandstones (Lent 1 and Ang B).

Structural Style: Rotated fault blocks associated with late stage salt withdrawal.

Trapping Mechanisms: Closure on upthrown side of faults; dip reversals and truncations.

Possible Hydrocarbon Source(s): Subjacent lower Tertiary slope mudstones.

Exploration Maturity: Mature.

Frontiers: Possible basinward extension of Glob a slope sandstones.

Limitations:

1. Largest structures have been tested.
2. Discontinuity of slope sandstones

Play 3

Hydrocarbon Type(s): Gas.

Defining Attribute(s): Progradational continental margin of Middle Pleistocene shelf-edge delta system and subjacent slope.

Reservoir Facies: Progradational and aggradational delta-front sandstones (Ang B and Hyal b).

Structural Style: Deep residual salt, folds, and extensional faults associated with salt withdrawal.

Trapping Mechanisms: Dip reversal and fault truncation.

Possible Hydrocarbon Source(s): Subjacent lower Tertiary slope mudstones.

Exploration Maturity: Mature.

Frontiers: Possible basinward extension of Glob a and Lent 1 slope sandstones.

Limitations:

1. Existing well density.
2. Basinward limit of sandstone deposition.

Play 4

Hydrocarbon Type(s): Gas.

Defining Attribute(s): Lower Pleistocene submarine fans and lowstand wedges.

Reservoir Facies: Progradational and aggradational upper slope sandstones (Lent 1 and Ang B).

Structural Style: Inversion of steeply dipping strata above glide plane and salt remnants.

Trapping Mechanisms: Combination structural and stratigraphic traps. Dip reversals and fault truncation against synthetic and antithetic faults.

Possible Hydrocarbon Source(s): Subjacent lower Tertiary slope mudstones.

Exploration Maturity: Mature.

Frontiers: Possible extension of Glob a and Lent 1 slope sandstones to the south and west.

Limitations:

1. Basinward limit of sandstone deposition.
2. Discontinuity of slope sandstones.

Play 5

Hydrocarbon Type(s): Gas.

Defining Attribute(s): Progradational continental margin of middle and late Pleistocene shelf-edge delta systems.

Reservoir Facies: Progradational and aggradational upper slope and delta-front sandstones (Hyal b and Trim A).

Structural Style: Graben complex formed by regional tensional stresses associated with salt migration.

Trapping Mechanisms: Prominent rollover between regional and counter-regional faults with minor antithetic faults.

Possible Hydrocarbon Source(s): Subjacent lower Tertiary slope mudstones.

Exploration Maturity: Mature.

Frontiers: Possible basinward extension of Ang B sandstones.

Limitations:

1. Largest structures have been tested.
2. Basinward limit of sandstone deposition.

Play 6

Hydrocarbon Type(s): Gas and some oil.

Defining Attribute(s): Upper Pleistocene sand-rich slope systems beneath modern slope.

Reservoir Facies: Progradational and aggradational middle slope sandstones (Hyal b and upper Trim A).

Structural Style: Large, isolated salt domes, counter-regional faults and intraslope basins.

Trapping Mechanisms: Truncation against counter-regional faults or against radial faults around salt domes.

Possible Hydrocarbon Source(s): Subjacent Cretaceous and lower Tertiary slope mudstones.

Exploration Maturity: Immature.

Frontiers: Entire play is sparsely drilled.

Limitations:

1. Water depths exceed 500 ft.
2. Variable extent of sandstone deposition.
3. Discontinuity of sandstone reservoirs.

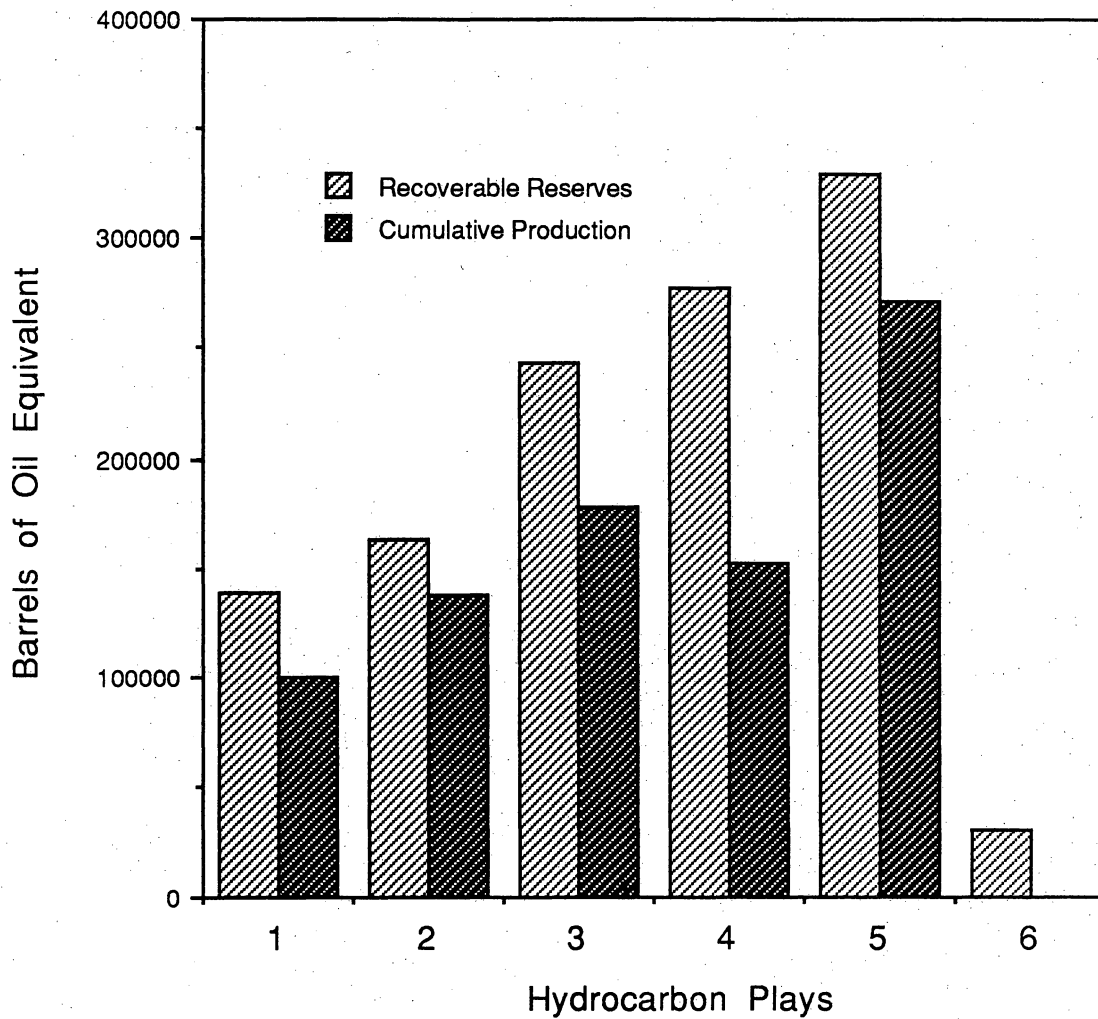


Figure 35. Cumulative production and recoverable reserves for each Plio-Pleistocene play in the West Cameron and western Garden Banks areas. Values for each play represent aggregated volumes for individual fields estimated by NRG Associates (1988).

NRG Associates (1988). Some field names designated in the NRG Associates database were combined or modified slightly (block numbers were merged) to agree with the list of offshore fields published by the Energy Information Administration (EIA, 1985).

Play Characteristics and Exploration Potential

Volumetric estimates of recoverable reserves were aggregated to quantify play richness and to provide additional criteria for defining play characteristics (fig. 35, Append.). Play 6, which currently contains slightly more than 30 million boe in discovered recoverable reserves, is the least productive play, but it is also the least explored play. In contrast, play 5 has slightly more than 329 million boe in 5 fields making it the richest play on the basis of total recoverable reserves. Play 4 is a close second in total recoverable reserves, having about 277 million boe in 6 fields. Plays 3 and 2 have about 243 million boe and 163 million boe in recoverable reserves respectively. Play 1 has about 138 million boe, but the gas is distributed in more than 28 fields that range in size from 1 million boe to 44 million boe (Append.).

The greatest concentration of hydrocarbons in the West Cameron South Addition area occurs in plays 3 and 4. Combined reserves for these two plays account for more than one-third of the total recoverable reserves in the study area (Append.). They also contain 4 of the 5 fields with the largest recoverable reserves. The concentration of recoverable reserves in a few medium size fields in plays 3, 4, and 5 indicates superior collection processes and efficient trapping mechanisms along a northeast-southwest trend that coincides with the subregional structural grain.

As of 1988, more than 830 million boe had been produced from Plio-Pleistocene reservoirs, representing approximately 73 percent of the total recoverable reserves (fig. 35, Append.). The ratio of cumulative production to recoverable reserves for each field varies greatly depending on such factors as date of field discovery, number of producing wells, and initial reserves. When aggregated by plays, substantial cumulative production is recorded for play 5 (271.7 million boe), representing 82 percent of recoverable reserves. Cumulative production from play 3 (177.1 million boe), play 4 (152.0 million boe), and play 2 (137.6 million boe) represents 73 percent, 55 percent, and 84 percent of recoverable reserves in each play, respectively (fig. 35). Only moderate volumes of hydrocarbons have been produced from play 1 (99.7 million boe), but they represent 72 percent of the recoverable reserves. Cumulative production is lowest in play 6 (unreported) because the fields are less than 10 yrs old, but at least one moderately large field (Garden Banks Block 189) is being developed. Play 5 has the largest fields and highest yield of any Plio-Pleistocene play in the study area, but play 6 has the greatest ultimate exploration potential because of the large number of untested structures (Table 1).

Hydrocarbon plays were delineated on the basis of available seismic and well control and actual field discoveries. The presence of Plio-Pleistocene deepwater sandstones having adequate reservoir properties and traces of oil basinward of the study area underscore the potential for additional commercial accumulations in play 6 beneath the modern slope (Foote and others, 1983). Although geological conditions are favorable for generating and trapping hydrocarbons in this deepwater frontier area, economic conditions and inventories of less speculative prospects in much shallower water may delay their exploitation.

Play 1

Play 1 encompasses a large area and contains a large number of hydrocarbon accumulations (fig. 33). Despite these favorable attributes, it has only moderate hydrocarbon exploration and production potential because of its structural and stratigraphic setting. Trap-forming structures are associated with shale ridges, widely-spaced growth faults, and a few salt spines (Table 1). These are mainly reactivated late Miocene structures that have caused relatively minor deformation of the Plio-Pleistocene strata (figs. 5-8). Play 1 contains the largest number of gas fields, but the fields are generally small (less than 20 million boe, Append.) because large growth faults or salt diapirs are absent. An exception is the West Cameron Block 280/281 field (field 5, fig. 33), which contains approximately 44 million boe and is the largest field in the play. The paucity of hydrocarbons in play 1, and in a comparable play in the High Island area (Morton and others, 1991), may be related to the hydrocarbon generating potential of the Tertiary source rocks and their maturation history.

Sandstone reservoirs occur in the Bul 1 (unit 1), Glob a (unit 2), and Lent 1 (unit 3) stratigraphic sequences. These sequences, which thicken basinward (figs. 5-8), were deposited on the preexisting upper Miocene continental slope. Outer shelf and upper slope delta-front facies of lowstand and transgressive systems tracts are the most promising reservoir rocks of the Plio-Pleistocene sequences.

Beneath play 1, middle-upper Miocene sediments are thick and composed mostly of slope mudstones interbedded with a few thin, discontinuous siltstones. Seismic profiles display numerous late Miocene structures such as rollover, dip reversal, and fault truncation that would act as hydrocarbon traps (figs. 5-8), but Miocene

sandbodies of reservoir quality are not present. This is because prolonged late Miocene and early Pliocene flooding of the continental platform caused deposition of transgressive systems tracts that progressively shifted the shoreline landward and caused the slope and shelf platform to be sites of mud deposition.

The density of exploration wells in play 1 is relatively low and the wells are concentrated on structural highs. Therefore, the greatest potential for additional reserves would be in small off-structure stratigraphic traps. Deeper drilling would provide one possible way of extending the play in limited downdip areas where the sand-prone Bul 1 and Glob a sequences remain untested.

Play 2

Prominent structural features and sedimentary facies define the geological limits of play 2 (Table 1). The basinward boundary of the play coincides with the basinward limit of thick Miocene deepwater shale and the Lent 1 shelf margin (figs. 5-8). Typical trap-forming structures are large growth faults, including upthrown sides of some growth faults (figs. 5, 7, and 8). Other hydrocarbon traps are created by minor faults along the Lent 1 shelf margin and prominent dip reversal associated with reactivated buried structures near the updip boundary of the play.

The largest fields in the play contain about 30 million boe (Append.). Several of the largest fields are concentrated in the southern and western parts of this play along an arcuate fault trend and near shallow salt diapirs (figs. 4 and 33). These deep-seated structures have been periodically reactivated and have also undergone late stage movement. Most of the structural deformation, however, coincided with Lent 1 deposition.

Hydrocarbon reservoirs in play 2 are mostly Lent 1 and Ang B progradational sandstones preserved near the top of each sequence. The reservoir rocks were deposited as highstand and transgressive systems tracts by shelf-edge and platform delta systems. Hydrocarbons are commonly trapped beneath the thick Lent 1 and Ang B transgressive shales, which act as reservoir seals. A few fields in play 2 produce from upward-coarsening parasequences near the base or middle part of each sequence that may represent lowstand systems tract deposits. In the West Cameron Block 464 and 547 fields, some gas has leaked into the overlying Hyal b sequence where it is trapped beneath the Hyal b shale in retrogradational sandstones of a transgressive systems tract.

It is possible that play 2 may be extended deeper if sand-rich Glob a slope aprons and submarine fans are present on the flanks of deep structures that were not bathymetric highs at the time of deposition. The risk of exploration in the area of possible play extension is increased by the abrupt lateral variations in lithofacies and greater potential of encountering slope mudstones rather than slope sandstones.

Play 3

The structural style of play 3 is characterized by large growth faults with substantial rollover and by the general absence of shallow piercement domes (figs. 4 and 33). Former salt structures were mobilized and evacuated in response to rapid slope aggradation and progradation of the Lent 1-Ang B (unit 4) continental platform (fig. 7) Moderately large shelf-edge deltas deposited thick successions of outer shelf and upper slope sediments as a lowstand wedge of the Cristellaria S interval (fig. 1) basinward of the Lent 1 shelf margin.

Play 3 produces gas from a few moderately large fields that contain as much as 102 million boe (Append.). These fields are associated with expansion of the Ang B section near the paleoshelf margin and in the adjacent salt withdrawal basins. Thick, vertically stacked, upward-coarsening sandstones deposited mainly by highstand and transgressive systems tracts serve as reservoirs. Some secondarily migrated gas accumulated in the overlying Hyal b (unit 5) and Trim A (unit 6) sandstones (fig. 7), also deposited by highstand and transgressive systems tracts. These leaked hydrocarbons are trapped beneath the Hyal b and Trim A transgressive shales, which act as the reservoir seals. Shallow gas in the Glob flex sequence also may have leaked from deeper reservoirs or may be of local biogenic origin.

Two different structural traps account for most of the fields in play 3. The first is faulted rollover anticlines downthrown on collapse faults that rim the northern perimeter of the play (figs. 4 and 33). The second type of trap occurs along the southern margin of the play on the hanging wall (upthrown) sides of faults where salt mobilization has caused structural inversion and created structural highs (figs. 7 and 8).

Deeper exploration for downdip pinchout of the Ang B sandstones represents one possible strategy for extending play 3. The potential for Glob a and Lent 1 sandstones on the flanks of intraslope basins provides additional exploration targets at depth (Table 1). Factors possibly limiting deeper play extension are: (1) the expected discontinuity of Glob a and Lent 1 slope sandstones and (2) the substantial drilling depths (> 10,000 ft) required to penetrate the objective section in the withdrawal basins.

Play 4

Play 4 is the eastern extension of play 3 (fig. 33) and therefore shares many of the same geological attributes such as the general absence of shallow salt diapirs, the presence of large growth-faults causing substantial basinward extension and stratigraphic throw, and the presence of a thick Cristellaria S lowstand wedge (figs. 5 and 6). A major difference between plays 3 and 4 is in the oldest producing stratigraphic sequence. In play 4, the Lent 1 sequence is thicker, contains more sand, and produces gas whereas it is thinner and non-productive in play 3. The boundary between plays 3 and 4 is imprecise because the Lent 1 correlation is equivocal in some wells. This stratigraphic uncertainty occurs where the Lent 1 fauna was reworked and redeposited with the Cristellaria S lowstand wedge. Thus, the reported faunal tops may indicate that wells penetrated the Lent 1 section when they actually stopped in the Cristellaria S lowstand wedge.

Fields are preferentially located around the periphery of play 4, which is defined by faults (figs. 4 and 33). Structural traps are mainly faulted crests of anticlines formed by rollover into the master listric fault, whereas stratigraphic traps occur in the Lent 1 submarine fans above the decollement (fig. 6). Numerous antithetic faults also create minor structural traps within the submarine fan complex.

Four stratigraphic sequences (units 3-6) produce gas in play 4. Oldest reservoirs are lowstand systems tracts (Lent 1 and lower Ang B) whereas the youngest are highstand and transgressive systems tracts. Field sizes range from one million boe to 150 million boe (Append.) and the play encompasses two of the three largest fields in the study area (fields 59 and 64, fig. 33, Append.).

Hydrocarbon reservoirs in play 4 typically are upper slope sandstones deposited by Lent 1 lowstand submarine fans. Sparse well control indicates that the underlying Glob a interval is mostly represented by slope mudstones, but some thin and highly discontinuous Glob a slope sandstones may have been deposited as a lowstand fan. In contrast, strata above the Lent 1 transgressive shale were deposited along an unstable shelf margin and later on a stable platform by moderately large shelf-edge deltas.

Additional deep drilling may encounter Glob a submarine fans or laterally extend the Lent 1 reservoirs in combination structural and stratigraphic traps near the center of the withdrawal syncline. This deep play extension involves greater risk because the slope sandstones are discontinuous and may be near the downdip limit of sandstone deposition (Table 1).

Play 5

Play 5 lies entirely within a series of moderately large withdrawal basins bounded by the Trimosina regional and counter-regional faults (figs. 4 and 33). This graben complex (figs. 7 and 8) formed while thick wedges of clastic sediments deposited at the Ang B and younger shelf margins displaced underlying salt; consequently, most salt structures within the play are deeply buried or absent. Large hydrocarbon traps were created by contemporaneous rollover into master faults and sedimentary downbuilding around residual salt masses. Some antithetic faults having small displacements at the anticlinal crests also serve as secondary hydrocarbon traps.

Gas reservoirs in play 5 are composed of thick upper-slope and delta-front sandstones deposited by highstand and transgressive systems tract shelf-edge deltas. The seals are overlying thick marine mudstones of the transgressive systems tract.

Play 5 contains more gas than any other West Cameron Plio-Pleistocene play (Append.) because of the large structural closures, proximity to deep-seated faults, and excellent seals.

Upper Trim A and middle Glob flex sandstones are primary exploration targets in play 5 (fig. 6). Secondary accumulations are present in Hyal b and Ang B sandstones (fig. 7). Some deep Lent 1 (sequence 3) submarine fans may be present in play 5; however, the variable extent of sandstones may limit their exploration potential. Exploration targets below sequence 3 are unattractive because the older sequences are primarily composed of deepwater mudstone (figs. 7 and 8).

Play 6

Play 6 is also defined on the basis of structural features and reservoir facies (Table 1). Prominent structural features are large, semi-continuous salt massifs and counter-regional faults that underwent recent movement (figs. 4 and 9). Most of the play is seaward of the extant shelf margin (fig. 33) where water depths range from a few hundred to more than 3,000 ft (900 m). It includes the western part of the Plio-Pleistocene flexure trend, which is an active exploration frontier in offshore Louisiana. The updip boundary of play 6 coincides with the Trimosina counter-regional fault zone (fig. 4 and 33). A southern boundary was not established because the basinward limit of sandstone deposition was not delineated by the available well logs.

Gas production in play 6 is mostly from upper Trim A slope sandstones deposited by lowstand and transgressive systems tracts. Hyal b and Ang B sand-rich fans are well developed in play 6 (fig. 21) and extend far downdip beyond the limit of well control. These lowstand fans are also potential hydrocarbon reservoirs that may produce from Garden Banks Block 191 (fig. 9).

Judging from recent discoveries to the east (Garden Banks area) and to the west (East Breaks area), play 6 may contain large reserves of gas and some oil. Average field size is uncertain because of the few discoveries (Append. and fig. 33), but undiscovered fields may be moderately large owing to the combination of large structural closures, trap-forming faults, presence of thick reservoir sandstones, and impermeable seals. Fields in play 6 are associated with faulted crests and flanks of shallow salt structures that have undergone relatively late movement, mostly coincident with Trim A or later deposition. Fields such as Garden Banks Block 192/236 (fig. 33, field 86) coincide with sand-trapping paleobathymetric lows that became structural highs as a result of late salt movement. Late hydrocarbon migration is also indicated by accumulations in the uppermost Trim A sandstones.

A significant new field discovery in Garden Banks Block 189 (fig. 33, field 85) reconfirms the presence of liquid hydrocarbons in the Plio-Pleistocene flexure trend along the upper slope. Initial tests of the discovery well in Block 189 indicated a production potential of 740 bbl of oil/day and 650 Mcf of gas/day.

The potential for new field discoveries in play 6 is excellent because the number of wells per unit area is extremely small and many large structures remain untested (Table 1). Economic considerations and geological limitations to future exploration in play 6 include deep water drilling sites, downdip limits of sandstone deposition for some stratigraphic units, discontinuity of slope feeder systems that become highly digitate in the northern part of the play, and the late structural movement possibly after hydrocarbon migration that would have liberated the previously trapped hydrocarbons.

SUMMARY AND CONCLUSIONS

Plio-Pleistocene depositional sequences of the West Cameron and western Garden Banks areas record major regressive and transgressive events that advanced the continental margin and simultaneously deformed the underlying salt. The depositional sequences responded to eustatic sea-level cycles that were controlled by expansion and contraction of large continental glaciers in North America. At least eight major regressive-transgressive genetic sequences are recognized on the basis of well log interpretations, paleontologic extinctions, and seismic stratal patterns. Each of these sequences is characterized by as many as three parasequence sets that are local responses to changes in sediment supply and rates of subsidence. Most of the major depositional episodes lasted between 900,000 yrs and 150,000 yrs with durations generally decreasing for successively younger cycles. Abrupt lowering of sea level about 3.0, 2.4, 1.6, and 0.8 Ma profoundly affected the Plio-Pleistocene stratigraphy and depositional systems.

Principal structural features influencing the thickness and attitude of Plio-Pleistocene sediments are large growth faults, shale diapirs, salt diapirs, and unconformities. Beneath the modern shelf, families of major faults having large displacements are oriented northwest-southeast or east-west, representing the shelf margin orientation as it advanced basinward. Ages of principal fault systems progressively decrease basinward except where salt migration extended the updip section and reactivated older fault systems. Structures related to deformation of mobile sediments occur in four contiguous areas. Shale ridges are prominent and shallow salt domes are rare in the southern part of the West Cameron area where sand-rich Plio-Pleistocene sediments are only moderately thick. In the adjacent West Cameron South

Addition area, thick sequences of Plio-Pleistocene sediments have caused the almost complete evacuation of salt. Shallow diapirs are absent and only thin salt sheets remain below the listric faults. On the modern slope, large salt diapirs are shallow and widely spaced. They form semi-continuous massifs and counter-regional faults, relieving the tensional stresses radiate from and interconnect the domes. Erosional unconformities are locally confined to the domes and salt-cored faults except for areally limited disconformities associated with failed paleo-shelf margins.

Plio-Pleistocene deposits record a thick, overall upward-shoaling succession, reflecting the progressive basinward advancement of the shelf margin and construction of the continental platform. This succession is punctuated by thin, upward-deepening units. Oldest strata are pelagic and hemipelagic mudstones and turbidite sandstones deposited on the middle and upper slope by lowstand submarine slope aprons. The sandy slope aprons were fed by small mud-dominated fluvial systems supplied by trunk streams flowing from the northwest and northeast. Repeated outbuilding and upbuilding of the continental platform continued as shelf-edge deltas prograded onto the former slope. As available accommodation space was filled, shallow-water deltas built a broad aggradational platform.

Major regressions initiated by falling sea level phases about 2.4 and 1.6 Ma were perhaps the most important depositional events in terms of shelf margin progradation, salt reorganization, fault generation, fault reactivation, and hydrocarbon entrapment. The youngest Plio-Pleistocene strata (younger than 1.4 Ma) are products of repeated progradation and retrogradation that occurred in response to rapid sea-level fluctuations. Minor entrenched valley systems were filled with aggradational fluvial and estuarine deposits and transgressive marine mudstones deposited across the former coastal plains. These sediments are volumetrically unimportant but geologically

significant components of the paralic deposits that accumulated landward of the shelf margin. Pathways of sand transport associated with principal fluvial systems and slope systems were locally altered by paleo-topographic and paleo-bathymetric highs that diverted currents. Similarly, locations of the largest fluvial-deltaic systems were influenced by antecedent topography and newly created accommodation space. Plio-Pleistocene sediments deposited near or above wavebase contain an unusually large fine-grained component preferentially preserved as a result of the fluvial dominance of mud-rich deltas. Furthermore, the high rates of subsidence and sedimentation allowed little time for wave reworking and removal of mud.

About 100 fields have been discovered in the western Louisiana sector of the Plio-Pleistocene trend. Hydrocarbons are produced at depths ranging from 1,500 to 14,000 ft (457 to 4270 m); however, most production comes from 6,000 to 10,000 ft (1830 to 3050 m). Most of the fields produce either dry gas or gas and condensate. A few fields produce minor amounts of oil in addition to gas. Most of the oil is produced from young reservoirs in fields beneath the present-day slope.

Plio-Pleistocene fields typically are small and contain less than 10 MMboe but a few large fields contain more than 100 MMboe. Largest fields are located near the largest deep-rooted faults. The faults acted as conduits for fluid movement from late Tertiary mudstones into more permeable Plio-Pleistocene reservoirs. Estimated recoverable reserves for these fields is slightly more than 1.1 billion boe. Lowstand slope aprons and lowstand wedges account for the largest volume of reserves, but highstand and transgressive systems tracts (youngest retrogradational phases of Trim A, Hyal b, and Ang B) also contain significant reserves.

Fields producing from Plio-Pleistocene strata are divided into six exploration plays on the basis of structural style, reservoir facies, and hydrocarbon composition. Fields in play 1 are small (< 20 MMboe) and produce mostly gas. The traps formed by fault truncation and stratigraphic pinchout. Reservoirs are primarily lowstand slope apron deposits that range in age from Bul 1 to Lent 1. Play 1 includes the largest number of Plio-Pleistocene fields or accumulations (26) but it also has the least structural deformation and lowest potential for large field discoveries.

Play 2 also encompasses a large number of fields or accumulations (22) that produce primarily from delta-front and slope sandstones of the Lent 1 and Ang B genetic sequences.

Play 3 is defined by a large area of salt withdrawal that accompanied extensive progradation of the continental platform. Shallow salt structures are rare in this play. Thick, upward-coarsening sandstones deposited by Ang B shelf-edge deltas serve as the primary gas reservoirs.

Play 4 is similar to play 3 in its structural setting. Shallow salt is absent and some production is from reservoirs deposited by Ang B shelf-edge deltas. A major difference, however, is the thick successions of Lent 1 slope sandstones that produce gas from combination structural and stratigraphic traps. Together plays 3 and 4 contain the highest concentration of hydrocarbons of all the strike-aligned fault bounded trends.

Play 5 encompasses the largest fields and produces from broad rollover anticlines. These structures formed in a graben complex created by tensional stresses between regional and counter-regional faults and antithetic faults between the Hyal b and Trim A shelf margins.

Play 6 produces gas and some oil from moderately large fields. Field size may be larger than average owing to the broad structural closures associated with growth faults and semicontinuous salt massifs. Play 6 has the lowest well density and greatest exploration potential of all the Plio-Pleistocene plays.

All six plays offer some potential for new field discoveries and reserve growth. Undiscovered shallow gas reserves are probably present in plays 1 and 2 as small accumulations along minor faults. Reserve additions in most of the other plays will probably come from deeper drilling of older structures and deep flanks of salt domes, and from stratigraphic traps on the margins of intraslope basins. The greatest exploration potential for significant oil and gas reserves is associated with play 6 where large structures remain untested. The most attractive prospects in play 6 occur where large salt diapirs have elevated post-Lent 1 slope sandstones to structurally high positions. Hydrocarbons should be trapped where structural inversion focused the migration of fluids and seals prevented leakage of petroleum to the surface.

ACKNOWLEDGMENTS

Partial financial support for this study was provided by an industrial associates group that included BP Exploration Inc., CNG Producing Company, Mobil Exploration and Producing US Inc., Oryx Energy Company, and Union Texas Petroleum. Fairfield Industries and Halliburton Geophysical Services made substantial contributions to the study by providing selected seismic lines. The study also benefitted from proprietary well logs and paleontological reports provided by the following companies: Amerada Hess Corporation, ARCO Oil and Gas Company, CNG Producing Company, Conoco Inc., Corpus Christi Oil and Gas Company, Elf Aquitaine Petroleum, Exxon Company USA, Forest Oil Corporation, Kerr-McGee Corporation, Louisiana Land and Exploration,

Marathon Oil Company, McMoRan Oil and Gas Company, Mesa Limited Partnership,
Oryx Energy Company, Pennzoil Exploration and Production Company, Phillips
Petroleum Company, Samedan Oil Corporation, Texas Gas and Exploration, Texaco
USA, Total-Minatome, and Union Texas Petroleum.

REFERENCES

- Amery, G. B., 1969. Structure of Sigsbee scarp: American Association of Petroleum Geologists Bulletin, v. 58, p. 2480-2482.
- Austin, J. M., 1988. West Cameron Block 587 field, offshore Louisiana: New Orleans Geological Society. Offshore Louisiana Oil and Gas Fields, v. 2, p. 225-230.
- Beard, J. H., Sangree, J. B., and Smith, L. A., 1982. Quaternary chronology, paleoclimate, depositional sequences, and eustatic cycles: American Association of Petroleum Geologists Bulletin, v. 66, p. 158-169.
- Bernard, H. A., and LeBlanc, R. J., 1965. Resume' of the Quaternary geology of the northwestern Gulf of Mexico province. in, Wright, H. E., Jr., and Frey, D. G., The Quaternary of the United States: Princeton University Press, p. 137-185.
- Berryhill, H. E., Jr., ed., 1987. Late Quaternary facies and structure, northern Gulf of Mexico: Interpretations from seismic data: American Association of Petroleum Geologists Studies in Geology No. 23, 289 p.
- Bouma, A. H., 1982. Intraslope basins in northwest Gulf of Mexico: a key to ancient submarine canyons and fans, in Watkins, J. S., and Drake, C. L., eds., Studies in continental margin geology: American Association of Petroleum Geologists Memoir 34, p. 567-581

Bouma, A. H., Normark, W. R., and Barnes, N. E., 1985, Submarine fans and related turbidite systems: Springer-Verlag, New York, 351 p.

Brown, L. F., Jr., and Fisher, W. L., 1977, Seismic-stratigraphic interpretation of depositional systems: Examples from Brazilian rift and pull-apart basins, in Payton, C. E., ed., Seismic stratigraphy-applications to hydrocarbon exploration: American Association of Petroleum Geologists Memoir 26, p. 213-248.

Bruce, C. H., 1973, Pressured shale and sediment deformation: mechanism for development of regional contemporaneous faults: American Association of Petroleum Geologists Bulletin, v. 57, p. 878-886.

Buffler, R. T., Worzel, J. L., and Watkins, J. S., 1978, Deformation and origin of the Sigsbee Scarp - lower continental slope, northern Gulf of Mexico: 10th Offshore Technology Conference, paper OTC 3217, p. 1425-1438.

Buffler, R. T., and Sawyer, D. S., 1985, Distribution of crust and early history, Gulf of Mexico basin: Gulf Coast Association of Geological Societies Transactions, v. 35, p. 333-344.

Caughey, C. A., 1975, Pleistocene depositional trends host valuable Gulf oil reserves: Oil and Gas Journal, v. 73, part 1, no. 36, p. 90-94; part 2, no. 37, p. 240-242.

Cochrane, J. D., and Kelly, F. J., 1986, Low-frequency circulation on the Texas-Louisiana continental shelf: *Journal of Geophysical Research*, v. 91, p. 10645-10659.

Coleman, J. M., Prior, D. B., and Lindsey, J. F., 1983, Deltaic influences on shelfedge instability processes, *in*, Stanley, D. J., and Moore, G. T., *The shelf break: critical interface on continental margins*: Society of Economic Paleontologists and Mineralogists Special Publication 33, p. 121-137.

Coleman, J. M., and Roberts, H. H., 1988, Sedimentary development of the Louisiana continental shelf related to sea level cycles: *Geo-Marine Letters*, v. 8, p. 63-119.

Crans, W., Mandl, G., and Haremboure, J., 1980, On the theory of growth faulting, a geomechanical delta model based on gravity sliding: *Journal of Petroleum Geology*, v. 2, p. 265-307.

Curtis, D. M., and Picou, E. B., 1978, Gulf Coast Cenozoic: a model for the application of stratigraphic concepts to exploration on passive margins: *Gulf Coast Association of Geological Societies Transactions*, v. 28, p. 103-120.

Dailly, G. C., 1976, A possible mechanism relating progradation, growth faulting, clay diapirism and overthrusting in a regressive sequence of sediments: *Bulletin of Canadian Petroleum Geology*, v. 24, p. 92-116.

Dinkleman, M. G., and Curry, D. J., 1987. Significance of anoxic slope basins to occurrence of hydrocarbons along flexure trend, Gulf of Mexico: a reappraisal: (abst.) American Association of Petroleum Geologists Bulletin, v. 71, p. 548.

Dow, W. G., 1978. Petroleum source beds on continental slopes and rises: American Association of Petroleum Geologists Bulletin, v. 62, p. 1584-1606.

Dow, W. G., and Pearson, D. B., 1975. Organic matter in Gulf Coast sediments: Seventh Offshore Technology Conference Preprints, paper OTC 2343, unpaginated.

Energy Information Administration, 1985. Oil and gas field code master list 1985: Office of Oil and Gas, U. S. Department of Energy, Washington D. C., 586 p.

Farre, J. A., McGregor, B. A., Ryan, W. B. F., and Robb, J. M., 1983. Breaching the shelfbreak: passage from youthful to mature phase in submarine canyon evolution, in, Stanley, D. J., and Moore, G. T., The shelf break: critical interface on continental margins: Society of Economic Paleontologists and Mineralogists Special Publication 33, p. 25-39.

Fisher, W. L., and McGowen, J. H., 1967. Depositional systems in the Wilcox Group of Texas and their relationship to occurrence of oil and gas: Gulf Coast Association of Geological Societies Transactions, v. 17, p. 105-125.

- Fisk, H. N., 1939. Depositional terrace slopes in Louisiana: *Journal of Geomorphology*, v. 2, p. 181-200.
- Fisk, H. N., 1944. Geological investigation of the alluvial valley of the lower Mississippi River: Mississippi River Commission, 78 p.
- Fisk, H. N., and McFarlan, E. Jr., 1955. Late Quaternary deltaic deposits of the Mississippi River: *Geological Society of America Special Paper* 62, p. 279-302.
- Foote, R. Q., Martin, R. G., and Powers, R. B., 1983. Oil and gas potential of the maritime boundary region in the central Gulf of Mexico: *American Association of Petroleum Geologists Bulletin*, v. 67, p. 1047-1065.
- Frakes, L. A., 1979. *Climates throughout geologic time*: Amsterdam, Elsevier, 310 p.
- Frazier, D. E., 1974. Depositional episodes: their relationship to the Quaternary stratigraphic framework in the northwestern portion of the Gulf basin: The University of Texas at Austin, Bureau of Economic Geology *Geological Circular* 74-1, 28 p.
- Galloway, W. E., 1989. Genetic stratigraphic sequences in basin analysis 1: architecture and genesis of flooding-surface bounded depositional units: *American Association of Petroleum Geologists Bulletin*, v. 73, p. 125-142.

- Gibbs, A. D., 1984, Structural evolution of extensional basin margins: Geological Society of London Journal, v. 141, p. 609-620.
- Hall, D. J., Cavanaugh, T. D., Watkins, J. S., and McMillan, K. J., 1983, The rotational origin of the Gulf of Mexico based on regional gravity data, in Watkins, J. S., and Drake, D. L., eds., Studies in continental margin geology: American Association of Petroleum Geology Memoir 34, p. 115-126.
- Haq, B. U., Hardenbol, J., and Vail, P. R., 1987, Chronology of fluctuating sea levels since the Triassic (250 million years ago to present): Science, v. 235, p. 1156-1167.
- Harding, T. P., and Lowell, J. D., 1979, Structural styles, their plate-tectonic habits, and hydrocarbon traps in petroleum provinces: American Association of Petroleum Geologists Bulletin, v. 63, p. 1016-1058.
- Hidle, G. M., and Wright, S. A., 1988, West Cameron Block 543 field, offshore Louisiana: New Orleans Geological Society Offshore Louisiana Oil and Gas Fields, v. 2, p. 219-224.
- Huc, A. Y., and Hunt, J. M., 1980, Generation and migration of hydrocarbons in offshore South Texas Gulf Coast sediments: Geochimica et Cosmochimica Acta, v. 44, 1081-1089.
- Jackson, M. P. A., and Talbot C. J., 1986, External shapes, strain rates, and dynamics of salt structures: Geological Society of America Bulletin, v. 97, p. 305-323.

Jackson, M. P. A., and Cramez, C., 1989, Seismic recognition of salt welds in salt tectonics regimes: Gulf Coast Section Society of Economic Paleontologists and Mineralogists 10th Annual Research Conference, Program and Extended Abstracts, p. 72-78.

Kastens, K. A., and Shor, A. N., 1985, Depositional processes of a meandering channel on Mississippi fan: American Association of Petroleum Geologists Bulletin, v. 69, p. 190-202.

Lehner, P., 1969, Salt tectonics and Pleistocene stratigraphy on continental slope of northern Gulf of Mexico: American Association of Petroleum Geologists Bulletin, v. 53, p. 2431-2479.

Loutit, T. S., Hardenbol, J., Vail, P. R., and Baum, G. R., 1988, Condensed sections: the key to age dating and correlation of continental margin sequences, in Wilgus, C. K., and others eds., Sea-level changes: an integrated approach: Society of Economic Paleontologists and Mineralogists, Spec. Pub. 42, p. 183-213.

McFarlan, E., Jr., and LeRoy, D. O., 1988, Subsurface geology of the late Tertiary and Quaternary deposits, coastal Louisiana and adjacent continental shelf: Gulf Coast Association of Geological Societies Transactions, v. 38, p. 421-433.

Martin, R. G., 1980, Distribution of salt structures in the Gulf of Mexico, map and descriptive text: U.S. Geological Survey Miscellaneous Field Studies Map MF-1213.

Milliken, K. L., 1985, Petrology and burial diagenesis of Plio-Pleistocene sediments northern Gulf of Mexico: unpub. Ph. D. dissertation, The University of Texas at Austin, 112 p.

Minerals Management Service, 1986, Physical oceanography of the Gulf of Mexico: Minerals Management Service, Gulf of Mexico OCS Regional Office Visual No. 7.

Mitchum, R. M., 1985, Seismic stratigraphic expression of submarine fans, in Berg, O. R., and Woolverton, D. G., Seismic stratigraphy II: American Association of Petroleum Geologists Memoir 39, p. 117-136.

Mitchum R. M., Jr., Vail, P. R., and Sangree, J. B., 1977, Seismic stratigraphy and global changes of sea level, part 6: stratigraphic interpretation of seismic reflection patterns in depositional sequences, in C. E. Payton, ed., Seismic stratigraphy-applications to hydrocarbon exploration: American Association of Petroleum Geologists Memoir 26, p. 117-133.

Morton, R. A., in press, Contrasting styles of late Neogene deep-water sandstone deposition, offshore Texas, in Miall, A. D., and Tyler, N., eds, The three dimensional facies architecture of terrigenous clastic sediments and its implications for hydrocarbon discovery and recovery: Society of Economic Paleontologists and Mineralogists Special Publication.

Morton, R. A., Jirik, L. A., and Galloway, W. E., 1988, Middle-upper Miocene depositional sequences of the Texas coastal plain and continental shelf: Geologic framework, sedimentary facies, and hydrocarbon plays: The University of Texas at Austin, Bureau of Economic Geology Report of Investigations 174, 40 p.

Morton, R. A., and Galloway, W. E., in press, Depositional, tectonic, and eustatic controls on hydrocarbon distribution in divergent margin basins - Cenozoic Gulf of Mexico case history, in Marine Geology Special Issue.

Morton, R. A., and Jirik, L. A., 1989, Structural cross sections, Plio-Pleistocene Series, southeastern Texas continental shelf: The University of Texas at Austin, Bureau of Economic Geology Cross Sections.

Morton, R. A., Sams, R. H., and Jirik, L. A., 1991, Plio-Pleistocene depositional sequences of the southeastern Texas continental shelf: geologic framework, sedimentary facies, and hydrocarbon distribution: The University of Texas at Austin, Bureau of Economic Geology, Report of Investigations 200, 90 p.

NRG Associates, 1988, The significant oil and gas fields of the United States: Colorado Springs, Colorado, computer database.

Nunn, J. A., and Sassen, R., 1986, The framework of hydrocarbon generation and migration, Gulf of Mexico continental slope: Gulf Coast Association of Geological Societies Transactions, v. 36, p. 257-262.

Palmer, A. R., 1983, The Decade of North American Geology 1983 geological time scale: *Geology*, v. 11, p. 503-504.

Perlmutter, M. A., 1985, Deep-water clastic reservoirs in the Gulf of Mexico: A depositional model: *Geo-Marine Letters*, v. 5, p. 105-112.

Pilger, R. H., Jr., and Angelich, M. T., 1984, Gravity anomalies west of 90 W longitude, *in*, Buffler, R. T., Locker, S. D., Bryant, W. R., Hall, S. A., and Pilger, R. H., Jr., eds., Gulf of Mexico, Atlas 6., Ocean Margin Drilling Program, Regional Atlas Series: Marine Science International, Woods Hole, MA., Sheet 2.

Poag, C. W., and Valentine, P. C., 1976, Biostratigraphy and ecostratigraphy of the Pleistocene basin, Texas-Louisiana continental shelf: *Gulf Coast Association of Geological Societies Transactions*, v. 26, p. 185-256.

Posamentier, H. W., Jarvey, M. T., and Vail, P. R., 1988, Eustatic controls on clastic deposition 1- Conceptual framework, *in* Wilgus, C. K., and others eds., Sea-level changes: an integrated approach: *Society of Economic Paleontologists and Mineralogists, Spec. Pub. 42*, p. 109-124.

Reed, J. C., Leyendecker, C. L., Khan, A. S., Kinler, C. J., Harrison, P. F. and Pickens, G. P., 1987, Correlation of Cenozoic sediments, Gulf of Mexico outer continental shelf: Minerals Management Service, OCS Report MMS 87-0026, alpha-numeric pagination.

Rezak, R., Bright, T. J., and McGrail, D. W., 1985, Reefs and banks of the northwestern Gulf of Mexico: John Wiley and Sons, New York, 259 p.

Rice, D. D., 1980, Chemical and isotopic evidence of the origins of natural gases in offshore Gulf of Mexico: Gulf Coast Association of Geological Societies Transactions, v. 30, p. 203-213.

Russell, R. J., 1940, Quaternary history of Louisiana: Geological Society of America Bulletin, v. 51, p. 1199-1233.

Sangree, J. B., and Widmier, J. M., 1977, Seismic stratigraphy and global changes of sea level, part 9: Seismic interpretation of clastic depositional facies, in C. E. Payton, ed., Seismic stratigraphy - applications to hydrocarbon exploration: American Association of Petroleum Geologists Memoir 26, p. 165-184.

Sangree, J. B., Waylett, D. C., Frazier, D. E., Amery, G. B., and Fennessy, W. J., 1978, Recognition of continental-slope seismic facies, offshore Texas-Louisiana, in Bouma, A. H., Moore, G. T., and Coleman, J. M., Framework, facies, and oil-trapping characteristics of the upper continental margin: American Association of Petroleum Geologists, Studies in Geology No. 7, p. 87-116.

Sasson, R., 1990, Lower Tertiary and upper Cretaceous source rocks in Louisiana and Mississippi - implications to Gulf of Mexico crude oil: American Association of Petroleum Geologists, v. 74, p. 857-878.

Sheffield, F. C., 1978, Where to next in the Gulf of Mexico? A brief review of future exploration opportunities in the Gulf: Proceedings of the 1978 Offshore Technology Conference, v. 1, p. 383-390.

Steffens, G. S., 1986, Pleistocene entrenched valley/canyon systems, Gulf of Mexico: (abst.) American Association of Petroleum Geologists Bulletin, v. 70, p. 1189.

Stuart, C. J., and Caughey, C. A., 1977, Seismic facies and sedimentology of terrigenous Pleistocene deposits in northwest and central Gulf of Mexico, in Payton, C. E., ed., Seismic stratigraphy-applications to hydrocarbon exploration: American Association of Petroleum Geologists Memoir 26, p. 249-275.

Stude, G. R., 1984, Neogene and Pleistocene biostratigraphic zonation of the Gulf of Mexico Basin: Proceedings Annual Research Conference, Gulf Coast Section Society of Economic Paleontologists and Mineralogists, p. 92-101.

Suter, J. R., and Berryhill, H. L., Jr., 1985, Late Quaternary shelf-margin deltas, northwest Gulf of Mexico: American Association of Petroleum Geologists Bulletin, v. 69, p. 77-91.

Thompson, K. M., Kennicutt, M. C. II, and Brooks, J. M., 1990, Classification of offshore Gulf of Mexico oils and gas condensates: American Association of Petroleum Geologists Bulletin, v. 74, p. 187-198.

Vail, P. R., Mitchum, R. M., Jr., and Thompson, S., III. 1977. Seismic stratigraphy and global changes of sea level, part 3: Relative changes of sea level from coastal onlap. in C. E. Payton, ed., Seismic stratigraphy-applications to hydrocarbon exploration: American Association of Petroleum Geologists Memoir 26, p. 63-81.

Van Wagoner, J. C., Posamentier, H. W., Mitchum, R. M., Vail, P. R., Sarg, J. F., Loutit, T. S. and Hardenbol, J., 1988. An overview of the fundamentals of sequence stratigraphy and key definitions. in Wilgus, C. K., and others eds., Sea-level changes: an integrated approach: Society of Economic Paleontologists and Mineralogists, Spec. Pub. 42, p. 39-45.

Watkins, J. S., Ladd, J. W., Buffler, R. T., Shaub, F. J., Houston, M. H., and Worzel, J. L., 1978. Occurrence and evolution of salt in deep Gulf of Mexico. in Bouma, A. H., Moore, G. T., and Coleman, J. M., Framework, facies, and oil-trapping characteristics of the upper continental margin: American Association of Petroleum Geologists Studies in Geology No. 7, p. 43-65.

White, D. A., 1980. Assessing oil and gas plays in facies-cycle wedges: American Association of Petroleum Geologists Bulletin, v.64, p. 1158-1178.

Winker, C. D., and Edwards, M. B., 1983. Unstable progradational clastic shelf margins: Society of Economic Paleontologists and Mineralogists Special Publication No. 33, p. 139-157.

Woodbury, H. O., Murray, I. B., Pickford, P. J., and Akers, W. H., 1973, Pliocene and Pleistocene depocenters outer continental shelf, Louisiana and Texas: American Association of Petroleum Geologists Bulletin, v.57, p. 2428-2439.

Woodbury, H. O., Spotts, J. H., and Akers, W. H., 1978, Gulf of Mexico continental-slope sediments and sedimentation, in Bouma, A. H., Moore, G. T., and Coleman, J. M., Framework, facies, and oil-trapping characteristics of the upper continental margin: American Association of Petroleum Geologists Studies in Geology No. 7, p. 117-137.

Young, Allen, Monaghan, P. H., and Schweisberger, R. T., 1977, Calculation of ages of hydrocarbons in oils - physical chemistry applied to petroleum geochemistry I: American Association of Petroleum Geologists Bulletin, v. 61, p. 573-600.

APPENDIX: Tabulation of Plio-Pleistocene fields by play.

1988 recoverable reserves and cumulative production are from NRG Associates database. Field identification (ID) numbers appear on figure 33.

PLIO-PLEISTOCENE RECOVERABLE RESERVES AND CUMULATIVE FIELD PRODUCTION

ID No.	Field Name	Recov Res 1988 Mboe	Cum Prod 1988 Mboe
Play 1			
1	West Cameron Blk 264	-	-
2	West Cameron Blk 265	11230	9233
3	West Cameron Blk 276	-	-
4	West Cameron Blk 277	-	-
5	West Cameron Blk 280	44700	37798
87	West Cameron Blk 285	-	-
6	West Cameron Blk 339	-	-
7	West Cameron Blk 353	21000	18782
8	West Cameron Blk 359	-	-
9	West Cameron Blk 364	1015	6
10	West Cameron Blk 367	-	-
11	West Cameron Blk 368	10330	1177
12	West Cameron Blk 369	-	-
13	West Cameron Blk 370	5620	810
14	West Cameron Blk 379	3000	257
15	West Cameron Blk 381	-	-
16	West Cameron Blk 391	1280	89
17	West Cameron Blk 406	10835	8959
18	West Cameron Blk 409	10330	8411
19	West Cameron Blk 414	-	-
20	West Cameron Blk 420	3560	753
21	West Cameron Blk 421	-	-
22	West Cameron Blk 425	-	-
23	West Cameron Blk 427	3565	2093
96	West Cameron Blk 433	-	-
24	West Cameron Blk 436	11800	11344
97	West Cameron Blk 437	-	-
25	West Cameron Blk 447	-	-
TOTAL		138265	99712
Play 2			
26	West Cameron Blk 456	-	-
27	West Cameron Blk 457/458	-	-
28	West Cameron Blk 459	8300	5703
29	West Cameron Blk 463	-	-
30	West Cameron Blk 464	14270	9277
31	West Cameron Blk 480	33855	31929
32	West Cameron Blk 487	-	-

33	West Cameron Blk 491	-	-
34	West Cameron Blk 492	-	-
35	West Cameron Blk 493	-	-
36	West Cameron Blk 498	21960	20054
37	West Cameron Blk 504	5640	3215
38	West Cameron Blk 507	21530	13445
46	West Cameron Blk 509	-	-
90	West Cameron Blk 508/509	-	-
39	West Cameron Blk 513	5530	5530
40	West Cameron Blk 518	-	-
41	West Cameron Blk 522/543	31250	30694
42	West Cameron Blk 523	-	-
43	West Cameron Blk 540	10725	9189
44	West Cameron Blk 541	-	-
45	West Cameron Blk 542	-	-
47	West Cameron Blk 547	9675	8552
TOTAL		162735	137588

Play 3

48	West Cameron Blk 537	31800	15022
49	West Cameron Blk 551	-	-
91	West Cameron Blk 561	-	-
50	West Cameron Blk 563/565	102570	69265
88	West Cameron Blk 564	-	-
94	West Cameron Blk 566	-	-
51	West Cameron Blk 566/570	-	-
92	West Cameron Blk 572	-	-
52	West Cameron Blk 573	2025	1193
53	West Cameron Blk 575/584	-	-
54	West Cameron Blk 586/595	12875	12239
55	West Cameron Blk 587	93673	79385
93	West Cameron Blk 589	-	-
56	West Cameron Blk 592	-	-
TOTAL		242943	177104

Play 4

57	West Cameron Blk 530	1000	93
58	West Cameron Blk 531	-	-
59	West Cameron Blk 533/EC 281	150200	126282
60	West Cameron Blk 534	-	-
61	West Cameron Blk 536	8650	4668
62	West Cameron Blk 552/560	3500	2343
63	West Cameron Blk 554	-	-
64	West Cameron Blk 556/EC 299	96000	6841
65	West Cameron Blk 575	-	-
66	West Cameron Blk 560	4070	2991
67	West Cameron Blk 576	13870	8810
68	West Cameron Blk 583	-	-
97	West Cameron Blk 599	-	-
69	West Cameron Blk 600	-	-
70	West Cameron Blk 601	-	-
TOTAL		277290	152028

Play 5

71	West Cameron Blk 597	-	-
72	West Cameron Blk 604	-	-
73	West Cameron Blk 612	-	-
74	West Cameron Blk 617	122160	115356
98	West Cameron Blk 618	-	-
100	West Cameron Blk 619	-	-
75	West Cameron Blk 620	38600	33592
76	West Cameron Blk 624	-	-
83	West Cameron Blk 628	38000	26150
77	West Cameron Blk 630/637	30450	17059
78	West Cameron Blk 633	-	-
79	West Cameron Blk 639	78600	54734
80	West Cameron Blk 643	52010	41874
81	West Cameron Blk 645	-	-
82	West Cameron Blk 648	-	-
TOTAL		329370	271706

Play 6

84	West Cameron Blk 661	-	-
89	West Cameron Blk 663	-	-
85	Garden Banks Blk 189	-	-
86	Garden Banks Blk 236	30000	-
TOTAL		30000	-